Fully Ir(III) tetrazolate soft salts: the road to white-emitting ion pairs

Valentina Fiorini,[a]* Andrea D'Ignazio,[a] Karen D. M. Magee,[b] Mark I. Ogden,[b] Massimiliano Massi,[b]* and Stefano Stagni [a]*

[a]*Department of Industrial Chemistry "Toso Montanari", University of Bologna, Viale Risorgimento 4, I-40136 Bologna, Italy*

[b] *Department of Chemistry, Curtin University, GPO Box U 1987, Perth, Australia, 6845*

Electronic Supplementary Information - ESI

General considerations. All the reagents and solvents were obtained commercially (e.g. Aldrich) and used as received without any further purification, unless otherwise specified. All the reactions were carried out under an argon atmosphere following Schlenk protocols. Where required, the purification of the Ir(III) complexes was performed via column chromatography with the use of neutral alumina as the stationary phase. ESI-mass spectra were recorded using a Waters ZQ-4000 instrument (ESI-MS, acetonitrile as the solvent). Nuclear magnetic resonance spectra (consisting of ^{1}H and ^{13}C) were always recorded using a Varian Mercury Plus 400 instrument (^{1}H, 400.1; ^{13}C, 101.0 MHz.) at room temperature. ^{1}H and ^{13}C chemical shifts were referenced to residual solvent resonances.

Photophysics. Absorption spectra were recorded at room temperature using a Perkin Elmer Lambda 35 UV/vis spectrometer. Uncorrected steady-state emission and excitation spectra were recorded on an Edinburgh FLSP920 spectrometer equipped with a 450 W xenon arc lamp, double excitation and single emission monochromators, and a Peltier-cooled Hamamatsu R928P photomultiplier tube (185–850 nm). Emission and excitation spectra were acquired with a cut-off filter (395 nm) and corrected for source intensity (lamp and grating) and emission spectral response (detector and grating) by a calibration curve supplied with the instrument. The wavelengths for the emission and excitation spectra were determined using the absorption maxima of the MLCT transition bands (emission spectra) and at the maxima of the emission bands (excitation spectra). Quantum yields (Φ) were determined using the optically dilute method by Crosby and Demas[i] at excitation wavelength obtained from absorption spectra on a wavelength scale [nm] and compared to the reference emitter by the following equation:[ii]

$$\phi_s = \phi_r \left[\frac{A_r(\lambda_r)}{A_s(\lambda_s)}\right]\left[\frac{I_r(\lambda_r)}{I_s(\lambda_s)}\right]\left[\frac{n_s^2}{n_r^2}\right]\left[\frac{D_s}{D_r}\right]$$

where A is the absorbance at the excitation wavelength (λ), I is the intensity of the excitation light at the excitation wavelength (λ), n is the refractive index of the solvent, D is the integrated intensity of the luminescence, and Φ is the quantum yield. The subscripts r and s refer to the reference and the sample, respectively. A stock solution with an absorbance > 0.1 was prepared, then two dilutions were obtained with dilution factors of 20 and 10, resulting in absorbances of about 0.02 and 0.08 respectively. The Lambert-Beer law was assumed to remain linear at the concentrations of the solutions. The degassed measurements were obtained after the solutions were bubbled for 10 minutes under Ar atmosphere, using a septa-sealed quartz cell. Air-

equilibrated $[Ru(bpy)_3]Cl_2/H_2O$ solution (Φ = 0.028)[iii] was used as reference. The quantum yield determinations were performed at identical excitation wavelengths for the sample and the reference, therefore deleting the $I(\lambda_r)/I(\lambda_S)$ term in the equation. Emission lifetimes (τ) were determined with the single photon counting technique (TCSPC) with the same Edinburgh FLSP920 spectrometer using pulsed picosecond LED (EPLED 360, fhwm < 800 ps) as the excitation source, with repetition rates between 1 kHz and 1 MHz, and the above-mentioned R928P PMT as detector. The goodness of fit was assessed by minimizing the reduced χ^2 function and by visual inspection of the weighted residuals. To record the 77 K luminescence spectra, the samples were put in quartz tubes (2 mm diameter) and inserted in a special quartz dewar filled with liquid nitrogen. The solvent used in the preparation of the solutions for the photophysical investigations was of spectrometric grade. Experimental uncertainties are estimated to be ±8% for lifetime determinations, ±20% for quantum yields, and ±2 nm and ±5 nm for absorption and emission peaks, respectively.

Ligand synthesis

Warning! Tetrazole derivatives are used as components for explosive mixtures.[iv] In this lab, the reactions described here were only run on a few grams scale and no problems were encountered. However, great caution should be exercised when handling or heating compounds of this type.

Following the general method reported by Koguro and coworkers,[vi] tetrazole ligands [H-**Tph**] 5-phenyl-1*H*-tetrazole, [H-**TphCN**] 4-(1*H*-tetrazol-5-yl)benzonitrile, and [H-**TPYZ**] 2-(1*H*-tetrazol-5-yl)pyrazine, were obtained in quantitative yield.

[**H-Tph**] ^{1}H-NMR (DMSO d^{6}, 400 MHz) δ (ppm) = 8.06 - 8.03 (m, 2H), 7.62 -7.60 (m, 3H). [**H-TphCN**] ^{1}H-NMR (DMSO d^{6}, 400 MHz) δ (ppm) = 8.06 (d, 2H, $J_{H\text{-}H}$ = 3.99 Hz) 8.31 (d, 2H, $J_{H\text{-}H}$ = 7.99 Hz). [**H-TPYZ**] ^{1}H-NMR, 400 MHz, DMSO-d^{6} δ (ppm) = 9.39 (m, 1H); 8.87 (m, 2H).

General Procedure for the Preparation of the Anionic $[Ir(L)_2]^-$ / $[F_2Ir(L)_2]^-$ Type Complexes

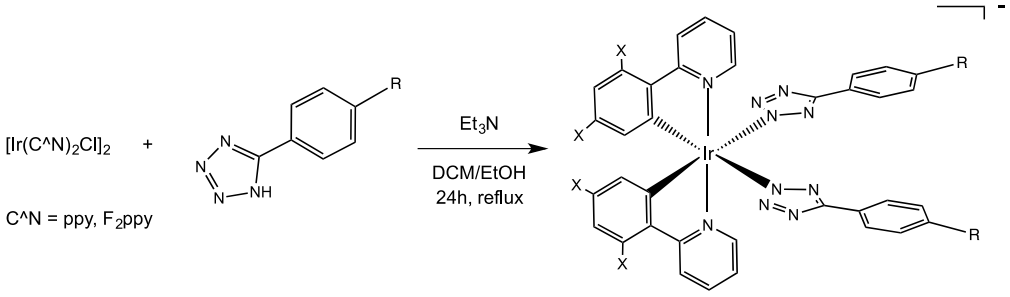

In a 50 mL two neck round bottom flask equipped with a stirring bar, 0.100 g (1 equiv.) of dichlorobridged iridium dimer and 10 equiv. of the desired tetrazole ligand were added to a 3:1 solution of dichloromethane/ethanol. Then, 10 equiv. of Et_3N were added, and the resulting mixture was stirred at reflux for 24 h. A 1:1 EP/Et_2O solution was added to the mother liquor and the respective products, bright yellow solids, precipitated from the solution, collected by filtration and washed with Et_2O (2x10 mL).

Yield: **$[Ir(Tph)_2]^-[Et_3NH]^+$** = 0.120 g; 72.1%. **$[F_2Ir(Tph)_2]^-[Et_3NH]^+$** = 0.133 g; 74.3%. **$[Ir(TphCN)_2]^-[Et_3NH]^+$** = 0.133 g; 0.152 mmol; 81.7%. **$[F_2Ir(TphCN)_2]^-[Et_3NH]^+$** = 0.104 g; 55.0%.

$[Ir(Tph)_2]^-$ ^{1}H-NMR (CD_3CN, 400 MHz) δ (ppm) = 6.41 (m, 2H), 6.69 (m, 2H), 6.76 (m, 2H), 7.31 (m, 2H), 7.36 (m, 4H), 7.44 (m, 2H), 7.59 (m, 2H), 7.85 (d, 4H, J_{H-H} = 5.6 Hz), 7.95 (m, 4H), 10.42 (d, 2H, J_{H-H} = 5.6 Hz). **^{13}C-NMR** (CD_3CN, 100 MHz) δ (ppm) = 168.52, 164.77, 153.34, 145.25, 137.06, 132.47, 131.07, 128.41, 128.38, 127.86, 126.00, 123.28, 121.81, 121.71, 120.55, 118.05. **ESI-MS** (*m/z*): [M^-] = 791; [M^+] = 102 (Et_3NH^+). Anal. Calcd. for $C_{42}H_{42}N_{11}Ir$ (893.07): C 56.48, H 4.74, N 17.25. Found: C 56.51, H 4.77, N 17.28%

$[F_2Ir(Tph)_2]^-$ ^{1}H-NMR (Acetone-d^6, 400 MHz) δ (ppm) = 5.97 (m, 2H), 6.35 (m, 2H), 7.25 (m, 2H), 7.30 (d, 4H, J_{H-H} = 7.9 Hz), 7.50 (m, 2H), 7.89 (d, 4H, J_{H-H} = 7.9 Hz), 8.04 (m, 2H), 8.26 (m, 2H), 10.51 (m, 2H).**^{13}C-NMR** (Acetone-d^6, 100 MHz) δ (ppm) = 165.03, 162.16, 153.81, 150.67, 137.88, 131.35, 128.22, 127.67, 125.99, 121.79, 121.62, 114.27, 114.10, 114.08, **ESI-MS** (*m/z*): [M^-] = 863; [M^+] = 102 (Et_3NH^+). Anal. Calcd. for $C_{42}H_{38}N_{11}F_4Ir$ (965.04): C 52.27, H 3.97, N 15.97. Found: C 52.25, H 3.99, N 16.00%

[Ir(TphCN)$_2$]$^-$ ^{1}H-NMR (Acetone-*d^6*, 400 MHz) δ (ppm) = 6.50 (m, 2H), 6.56 (m, 2H), 6.64 (m, 2H), 7.39 (m, 2H), 7.54 (m, 2H), 7.67 (d, 4H, $J_{H\text{-}H}$ = 7.9 Hz), 7.91 (m, 2H), 7.99 (m, 2H), 8.04 (d, 4H, $J_{H\text{-}H}$ = 7.6 Hz), 10.57 (m, 2H). **^{13}C-NMR** (Acetone-*d^6*, 100 MHz) δ (ppm) = 169.98, 161.52, 154.71, 146.17, 137.52, 136.37, 133.63, 133.02, 128.91, 127.17, 123.91, 121.99, 120.96, 119.17, 118.58, 111.19. **ESI-MS** (*m/z*): [M$^-$] = 841; [M$^+$] = 102 (Et_3NH^+). Anal. Calcd. for $C_{44}H_{40}N_{13}Ir$ (943.09): C 56.04, H 4.28, N 19.31. Found: C 56.08, H 4.30, N 19.29%

[F$_2$Ir(TphCN)$_2$]$^-$ ^{1}H-NMR (Acetone-*d^6*, 400 MHz) δ (ppm) = 5.95 (m, 2H), 6.35 (m, 2H), 7.51 (m, 2H), 7.69 (d, 4H, $J_{H\text{-}H}$ = 7.9 Hz), 7.76 (m, 2H), 8.04 (d, 4H, $J_{H\text{-}H}$ = 7.6 Hz), 8.35 (m, 2H), 10.45 (m, 2H). **^{13}C-NMR** (Acetone-*d^6*, 100 MHz) δ (ppm) = 166.03, 161.94, 154.66, 151.54, 138.87, 136.66, 133.97, 133.17, 133.14, 129.72, 127.55, 127.27, 127.24, 122.77, 119.57, 115.01, 111.57. **ESI-MS** (*m/z*): [M$^-$] = 913; [M$^+$] = 102 (Et_3NH^+). Anal. Calcd. for $C_{44}H_{36}N_{13}F_4Ir$ (1015.05): C 52.06, H 3.57, N 17.94. Found: C 52.04, H 3.59, N 17.97%

General Procedure for the Preparation of the Cationic Ir(III) complex

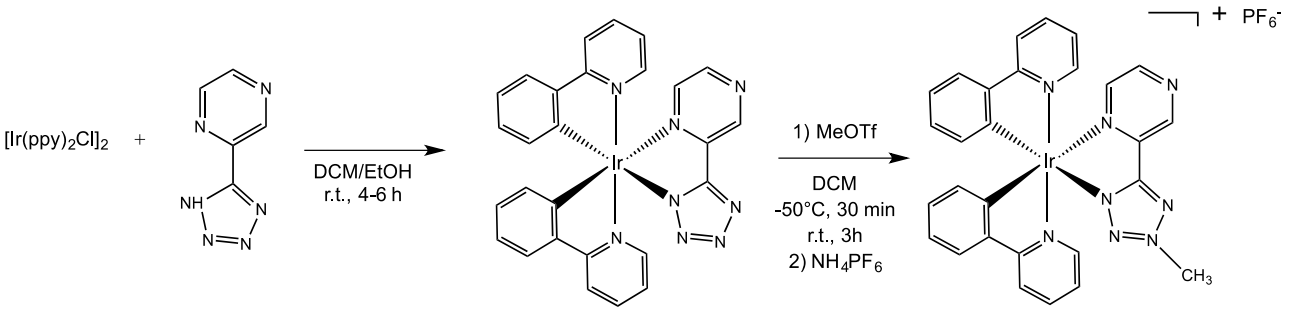

[IrTPYZ-Me]$^+$[PF$_6$]$^-$ was obtained according to a previously reported procedure.[vii] Yield: 0.038 g, 61.5%.

[IrTPYZ-Me]$^+$ ^{1}H-NMR (Acetone-*d^6*, 400 MHz) δ (ppm) = 9.76 (s, 1H), 8.99 (m, 1H), 8.26 (d, 2H, $J_{H\text{-}H}$ = 8.8 Hz), 8.11 (s, 1H), 8.02 – 7.95 (m, 3H), 7.91 – 7.85 (m, 3H), 7.15 – 6.85 (m, 6H), 6.32 – 6.27 (m, 2H), 4.61 (s, 3H). **^{13}C-NMR** (CD_3CN, 100 MHz) δ (ppm) = 168.48, 168.18, 166.55 (Ct), 152.62, 151.90, 151.52, 147.39, 146.72, 146.38, 145.74, 145.69, 145.30, 141.25, 140.51, 133.14, 132.77, 131.93, 131.36, 126.41, 125.98, 125.26, 125.11, 124.80, 124.38, 121.51, 121.28, 118.81, 43.47. **ESI-MS** (*m/z*): [M$^+$] = 663 [M$^-$] = 145 (PF_6). Anal. Calcd. for $C_{28}H_{22}N_8F_6PIr$ (807.71): C 41.63, H 2.75, N 13.87. Found: C 41.62, H 2.77, N 13.89%

General Procedure for the Preparation of Ir(III) Soft Salts

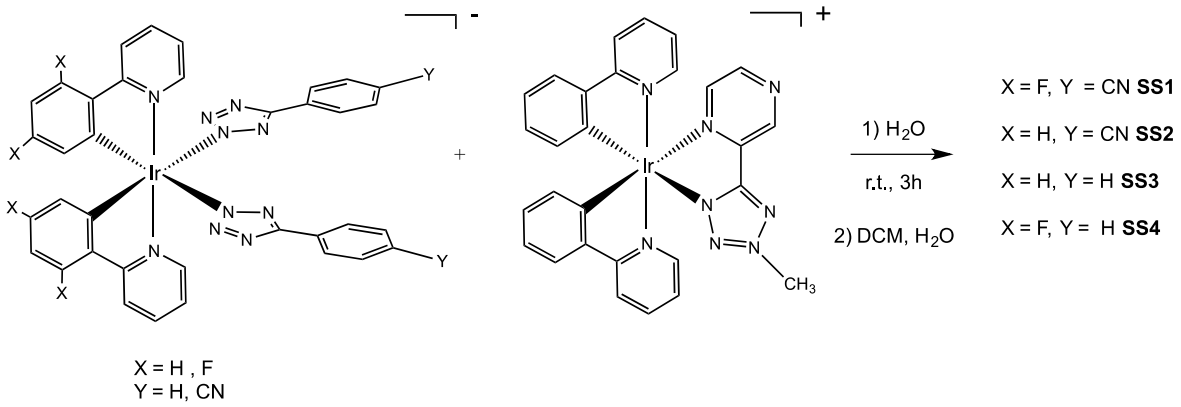

The desired anionic tetrazolate complex (0.020 g, 1 equiv.) and the proper cationic tetrazolate complex (1 equiv.) were added to water (15 mL). The reaction mixture was stirred for 3 h at room temperature and then extracted with dichloromethane. The organic phase was washed repeatedly with water until the signal of the counterion Et_3NH^+ was absent in the ^{1}H-NMR spectrum, leading to the formation of the Ir(III) soft salt in almost quantitative yield.

Table S1: Acronyms used for the presented Ir(III) Soft Salts.

Cation / *Anion*	**[IrTPYZ-Me]$^+$**
[F_2Ir(TphCN)$_2$]$^-$	**SS1**
[Ir(TphCN)$_2$]$^-$	**SS2**
[Ir(Tph)$_2$]$^-$	**SS3**
[F_2Ir(Tph)$_2$]$^-$	**SS4**

SS1 ^{1}H-NMR (CD_3CN, 400 MHz), δ (ppm): 4.47 (s, 3H cation), 5.86-5.89 (m, 2H, anion); 6.22-6.28 (m, 2H, cation), 6.37-6.43 (m, 2H, anion), 6.87-7.12 (m, 8H anion and cation overlapped), 7.45-7.48 (m, 2H, anion), 7.65-8.08 (m, 17H, anion and cation overlapped), 8.26-8.28 (m, 2H, anion), 8.78 (s, 1H, cation), 9.62 (s, 1H, cation), 10.21 (m, 2H, anion). Anal. Calcd. for $C_{66}H_{42}N_{20}F_4Ir_2 \bullet 2H_2O$ (1611.63): C 49.18, H 2.88, N 17.38. Found: C 49.25, H 2.85, N 17.42%

SS2 **^{1}H-NMR** (CD_3CN, 400 MHz), δ (ppm): 4.47 (s, 3H cation), 6.22-6.26 (m, 2H, cation); 6.40-6.43 (m, 2H, anion), 6.65-6.69 (m, 2H, anion), 6.74-6.78 (m, 2H, anion), 6.89-7.12 (m, 8H anion and cation overlapped), 7.41-7.44 (m, 2H, anion), 7.57-8.01 (m, 17H, anion and cation overlapped), 8.07-8.10 (m, 2H, anion), 8.78 (s, 1H, cation), 9.63 (s, 1H, cation), 10.34 (m, 2H, anion). Anal. Calcd. for $C_{66}H_{46}N_{20}Ir_2 \bullet 2H_2O$ (1539.67): C 51.48, H 3.27, N 18.19. Found: C 51.51, H 3.25, N 18.21%

SS3 **^{1}H-NMR** (CD_3CN, 400 MHz), δ (ppm): 4.47 (s, 3H, cation), 6.22-6.27 (m, 2H, cation), 6.41-6.44 (2H, anion), 6.64-6.68 (m, 2H, anion), 6.73-6.78 (m, 2H, anion), 6.87-7.12 (m, 6H, cation), 7.27-7.45 (m, 8H anion), 7.56-7.58 (m, 2H, anion), 7.64-7.67 (m, 2H cation), 7.72-7.98 (m, 13H, anion and cation overlapped), 8.07-8.09 (m, 2H, anion), 8.78 (s, 1H, cation), 9.63 (s, 1H, cation), 10.45 (m, 2H, anion). Anal. Calcd. for $C_{64}H_{48}N_{18}Ir_2 \bullet 2H_2O$ (1489.65): C 51.60, H 3.52, N 16.92. Found: C 51.63, H 3.54, N 16.95%

SS4 **^{1}H-NMR** (CD_3CN, 400 MHz), δ (ppm): 4.47 (s, 3H, cation), 5.87-5.90 (m, 2H anion), 6.22-6.27 (m, 2H, cation), 6.36-6.42 (m, 2H anion), 6.87-7.12 (m, 6H, cation), 7.29-7.49 (m, 8H anion), 7.65-7.67 (m, 2H, cation), 7.77-8.09 (m, 13H, anion and cation overlapped), 8.26-8.28 (m, 2H anion), 8.78 (s, 1H, cation), 9.62 (s, 1H, cation), 10.32 (m, 2H, anion). (Anal. Calcd. for $C_{64}H_{44}N_{18}F_4Ir_2 \bullet 2H_2O$ (1561.61): C 49.22 H 3.10, N 16.14. Found: C 49.26, H 3.05, N 16.18%

NMR and ESI-MS Spectroscopy

Figure S1: ^{1}H-NMR of **[Ir(Tph)$_2$]$^-$** CD_3CN, 400 MHz, r.t.

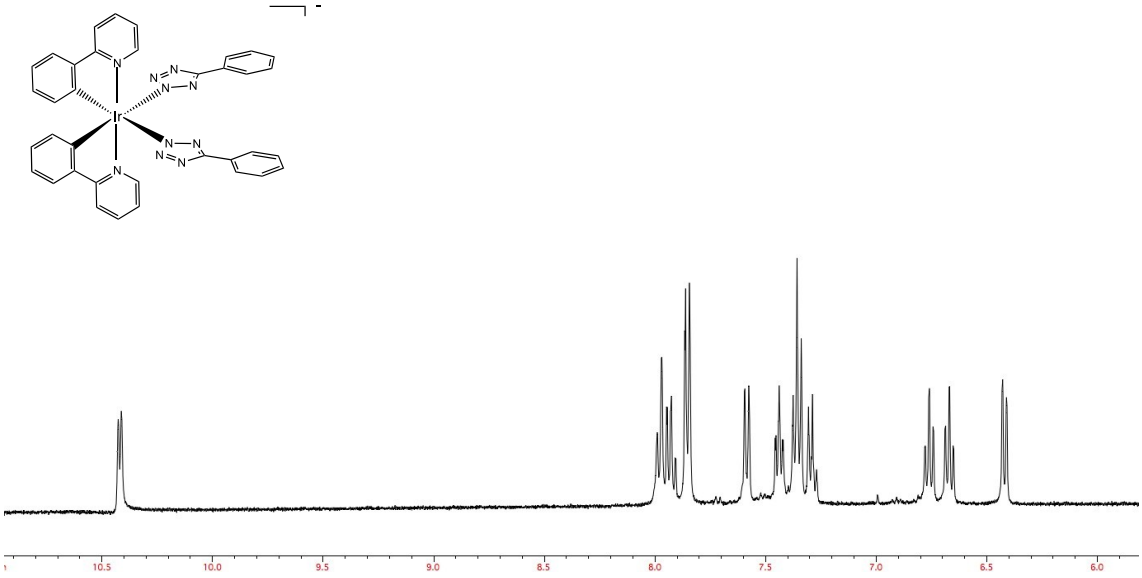

Figure S2: ^{13}C-NMR of **[Ir(Tph)$_2$]$^-$** CD_3CN, 400 MHz, r.t.

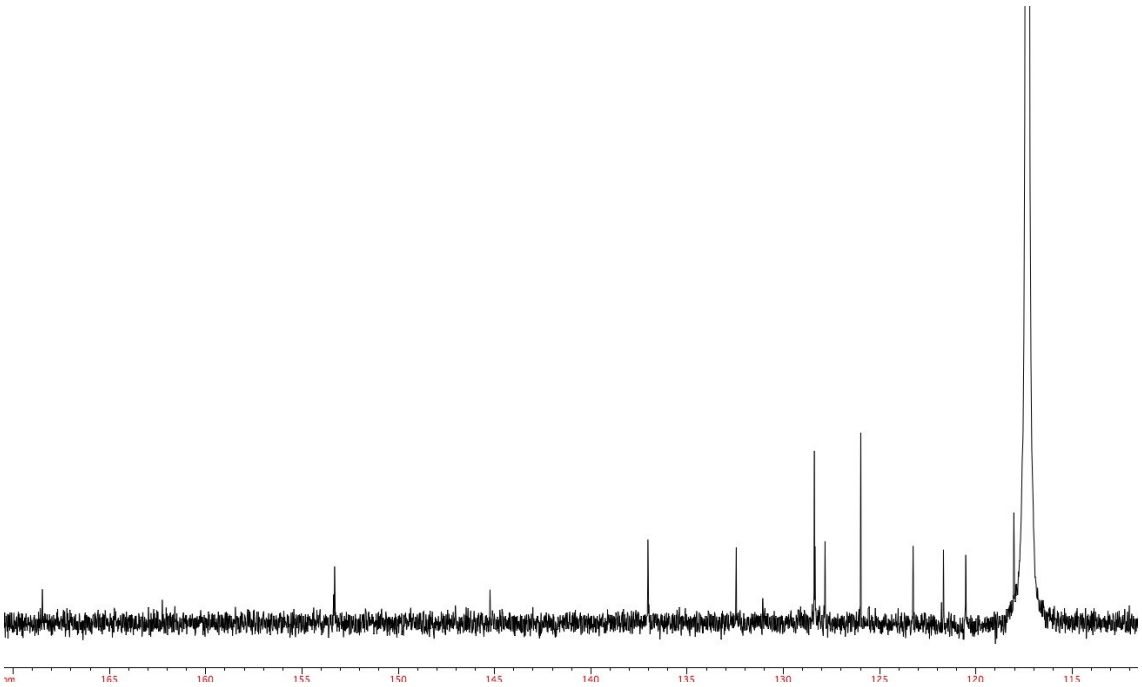

Figure S3: ^{1}H-NMR of **[F_2Ir(Tph)$_2$]**$^{-}$ Acetone-*d*^{6}, 400 MHz, r.t.

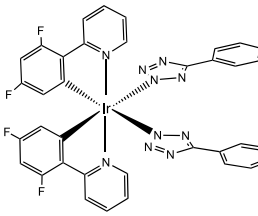

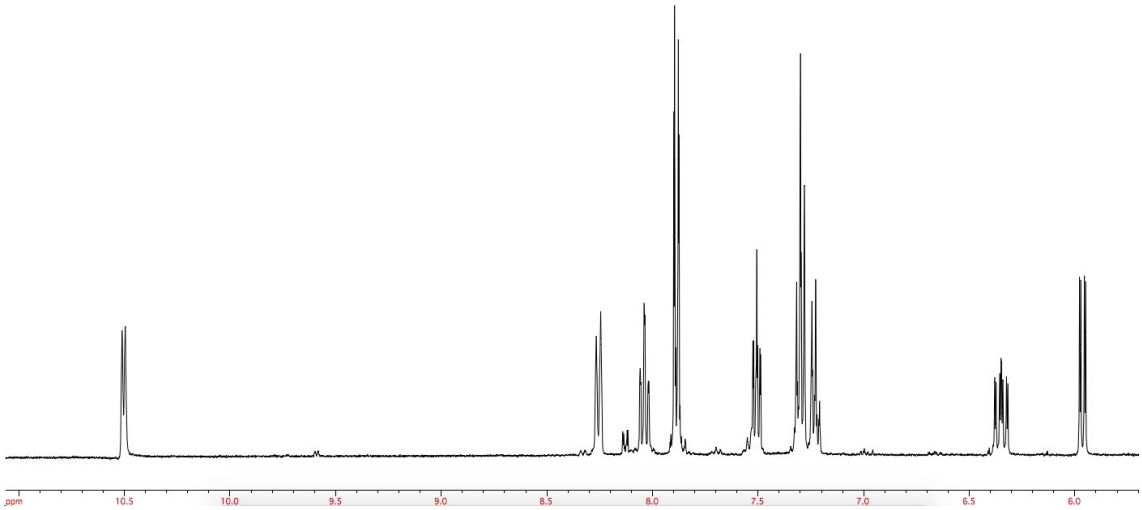

Figure S4: ^{13}C-NMR of **[F_2Ir(Tph)$_2$]**$^{-}$ Acetone-*d*^{6}, 100 MHz, r.t.

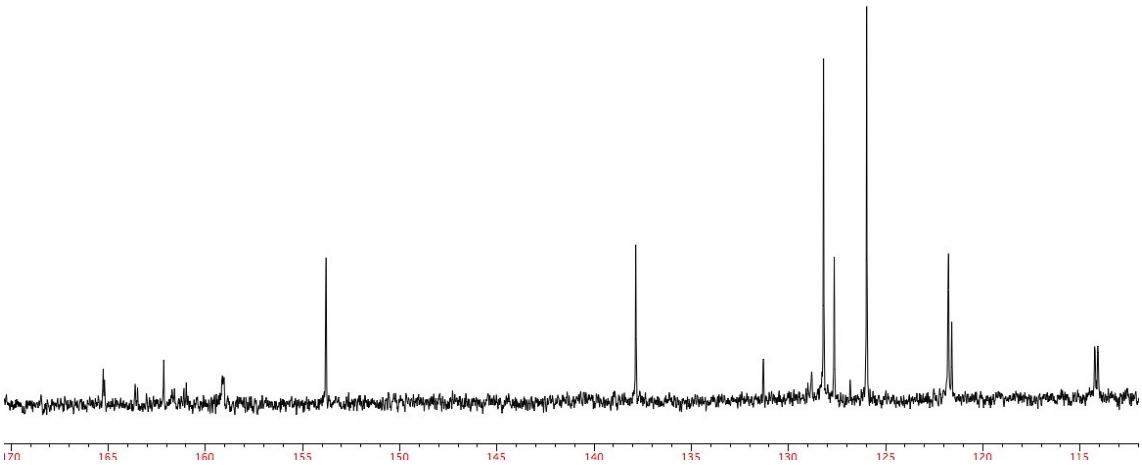

Figure S5: ^{1}H-NMR of **[Ir(TphCN)$_2$]$^-$** Acetone-*d*^{6}, 400 MHz, r.t.

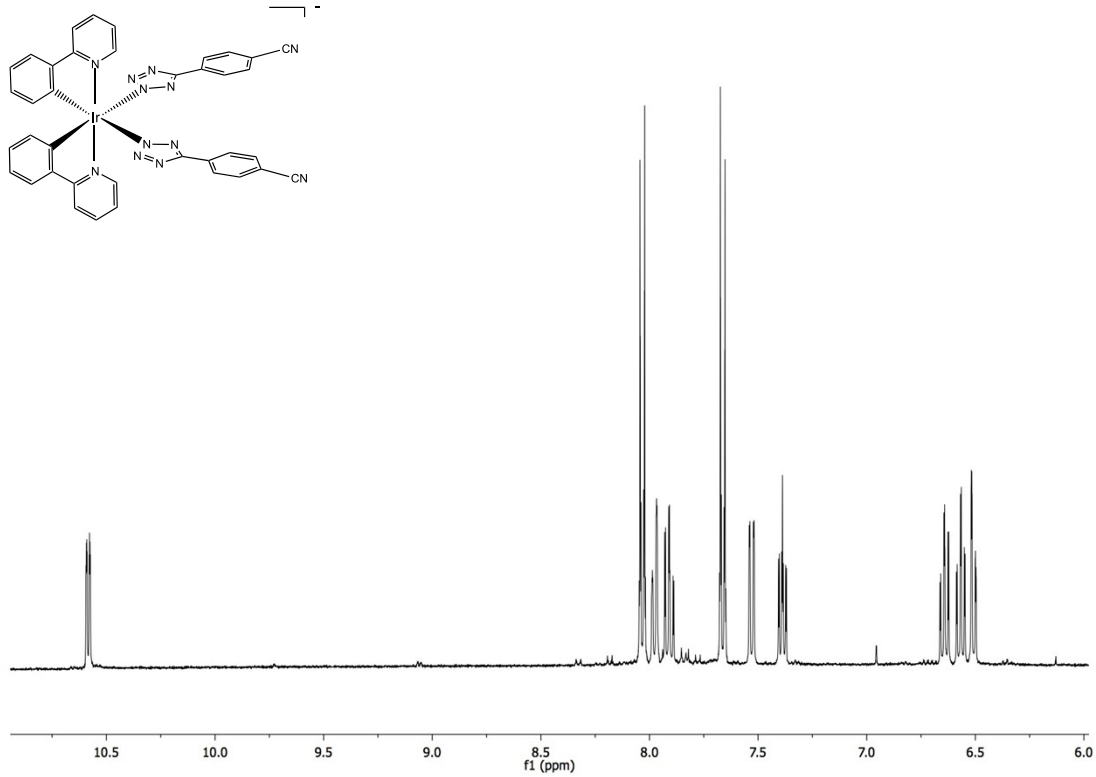

Figure S6: ^{13}C-NMR of **[Ir(TphCN)$_2$]$^-$** Acetone-*d*^{6}, 100 MHz, r.t.

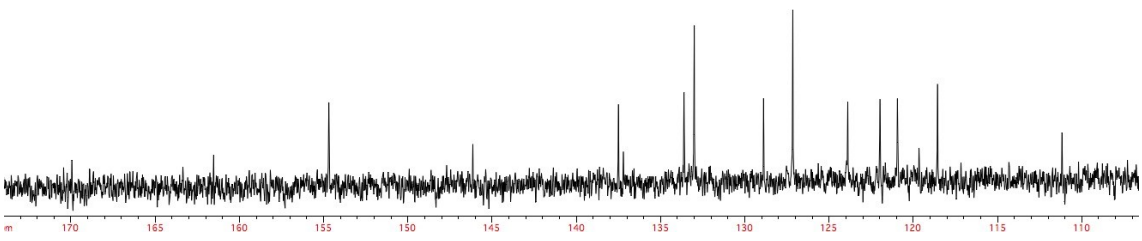

Figure S7: ^{1}H-NMR of **[F_2Ir(TphCN)$_2$]**$^{-}$ Acetone-*d*^{6}, 400 MHz, r.t.

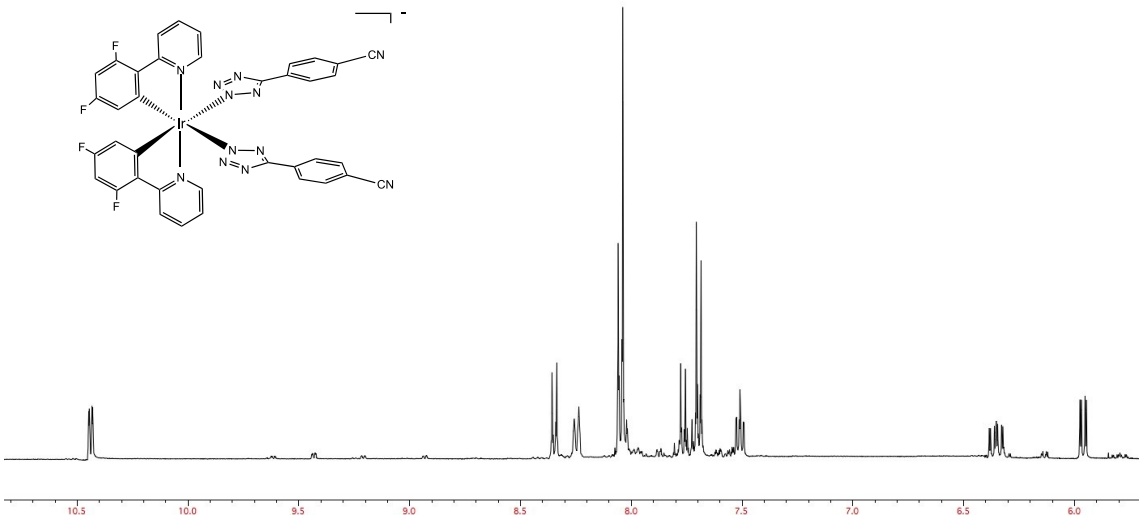

Figure S8: ^{13}C-NMR of **[F_2Ir(TphCN)$_2$]**$^{-}$ Acetone-*d*^{6}, 100 MHz, r.t.

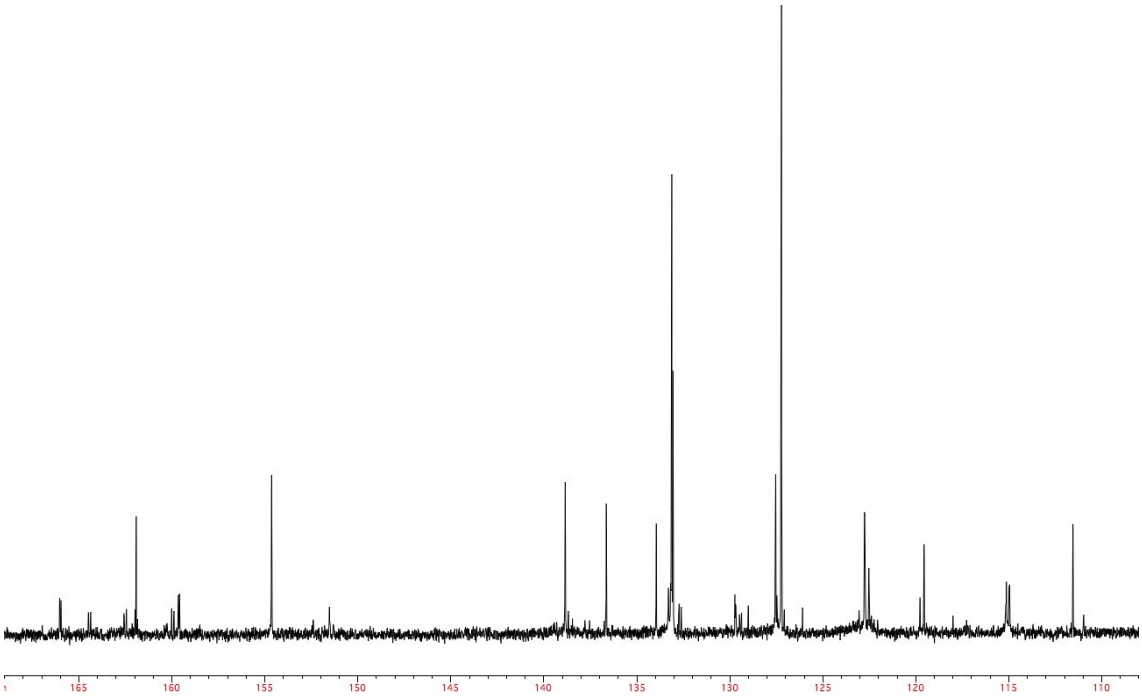

Figure S9: ^{1}H-NMR **[IrTPYZ-Me]$^{+}$** Acetone-*d*^{6}, 400 MHz, r.t.

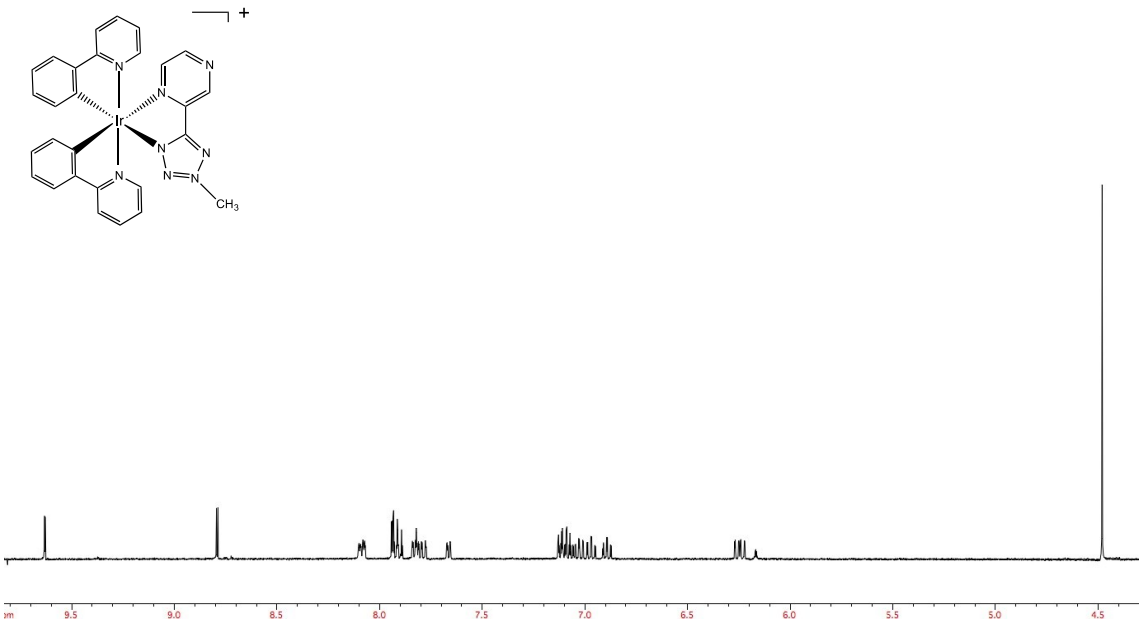

Figure S10: ^{13}C-NMR **[IrTPYZ-Me]$^{+}$** CD_3CN, 100 MHz, r.t.

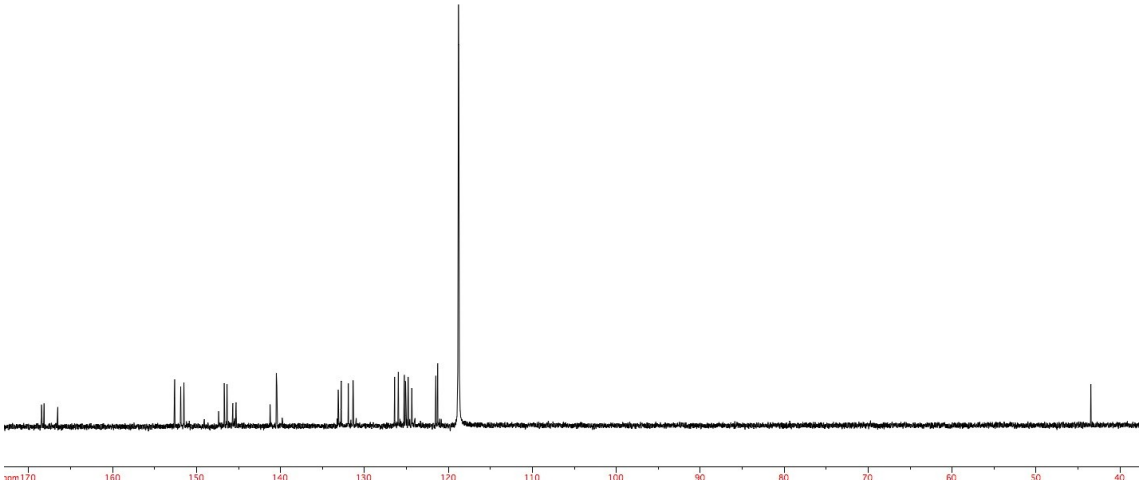

Figure S11: ^{1}H-NMR **SS1** CD_3CN, 400 MHz, r.t.

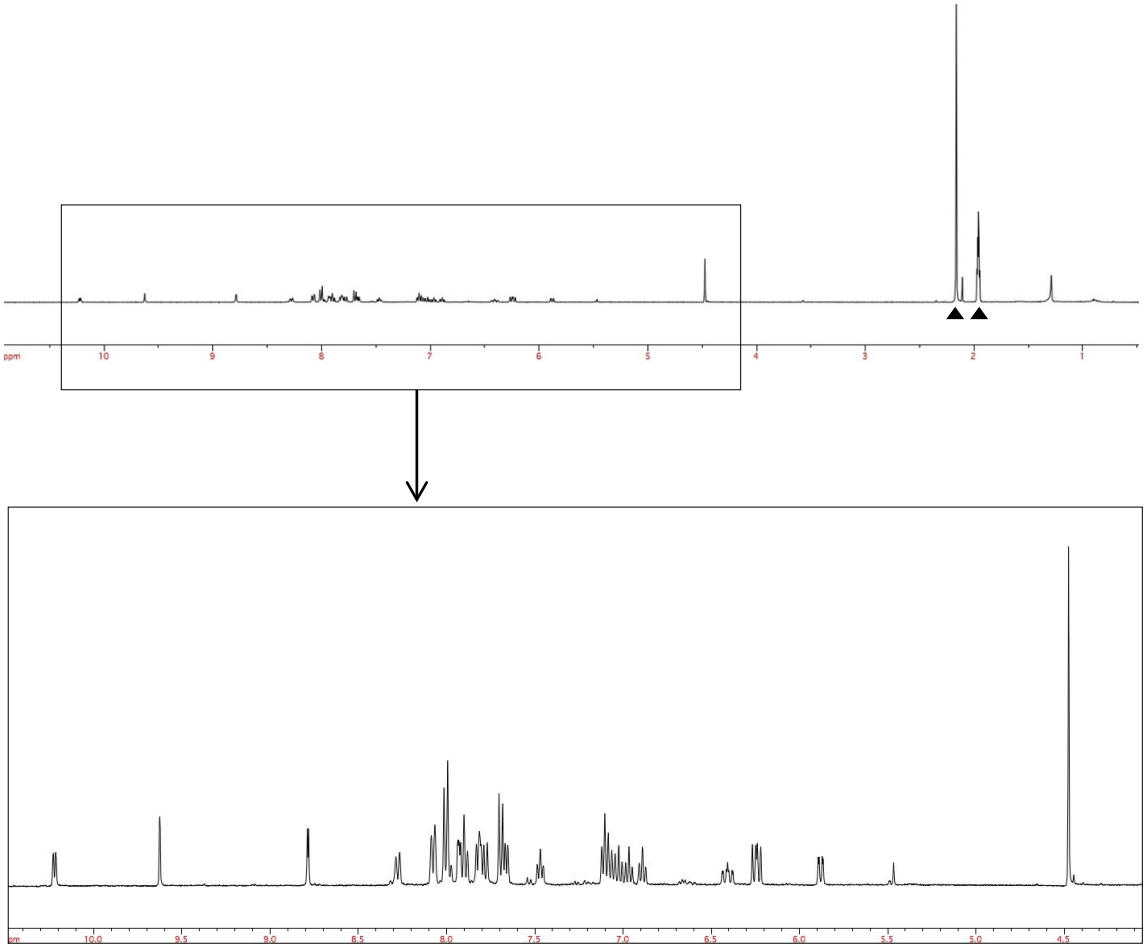

▲= ^{1}H signals of residual of non deuterated CD_3CN and water.

Figure S12: ^{1}H-NMR **SS2** CD_3CN, 400 MHz, r.t.

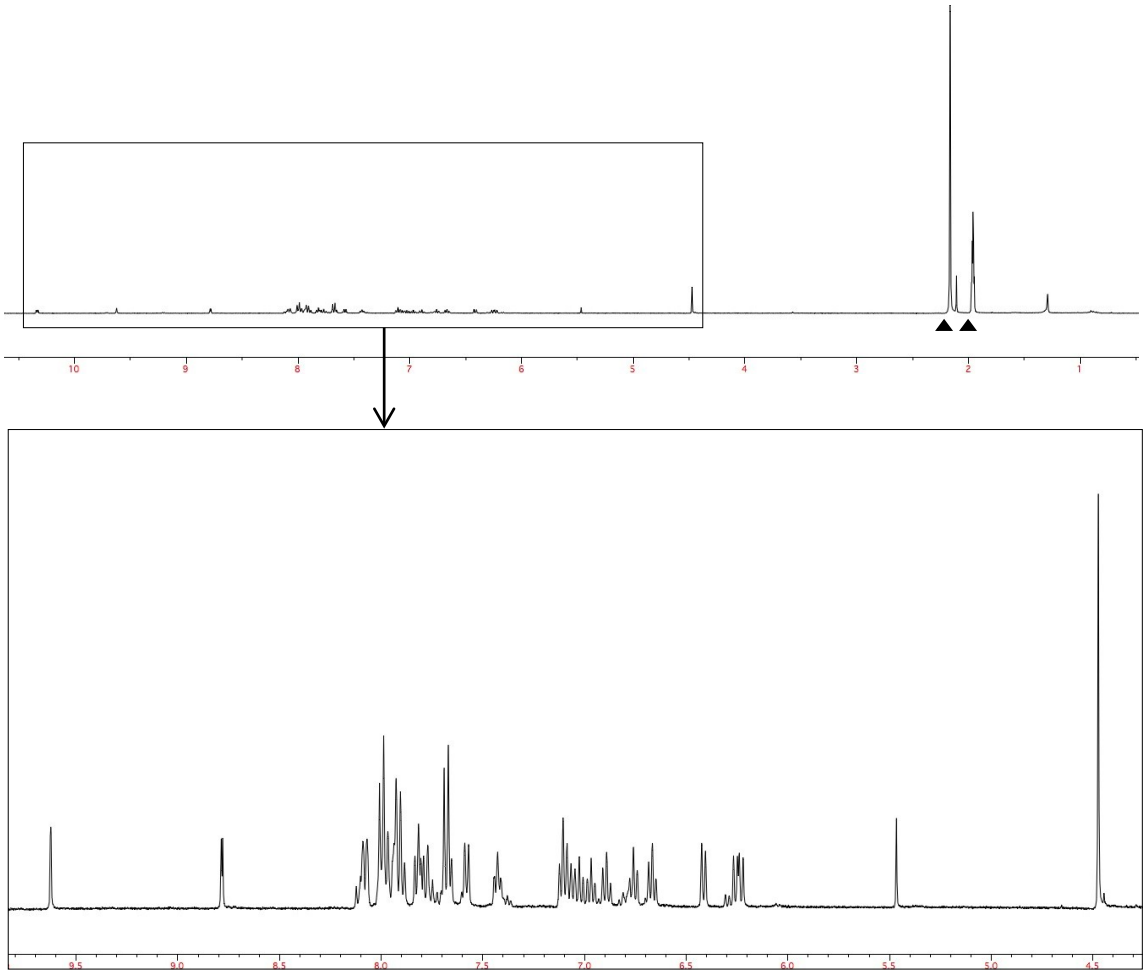

▲= ^{1}H signals of residual of non deuterated CD_3CN and water.

Figure S13: ^{1}H-NMR **SS3** CD_3CN, 400 MHz, r.t.

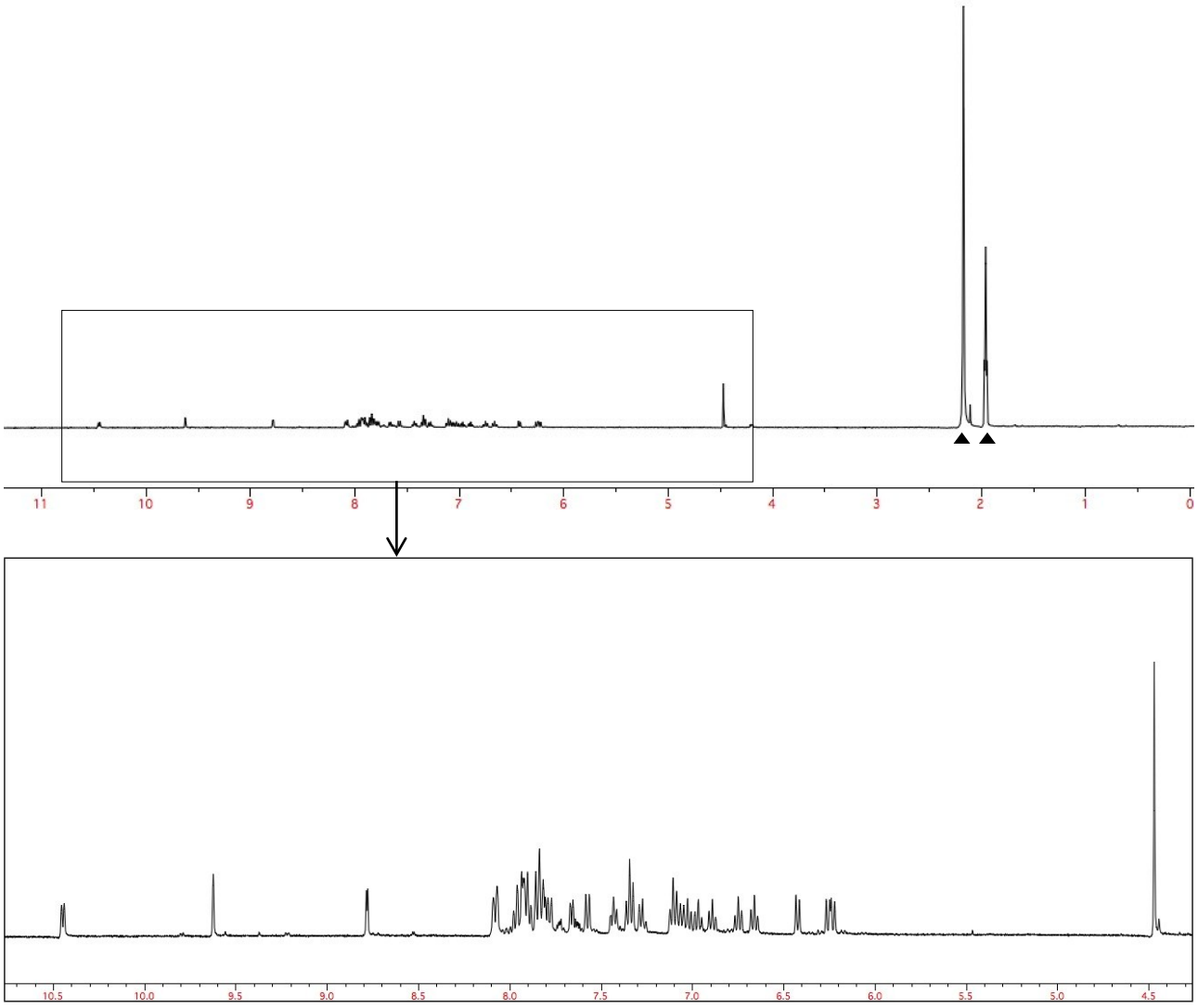

▲= ^{1}H signals of residual of non deuterated CD_3CN and water.

Figure S14: ^{1}H-NMR **SS4** CD_3CN, 400 MHz, r.t.

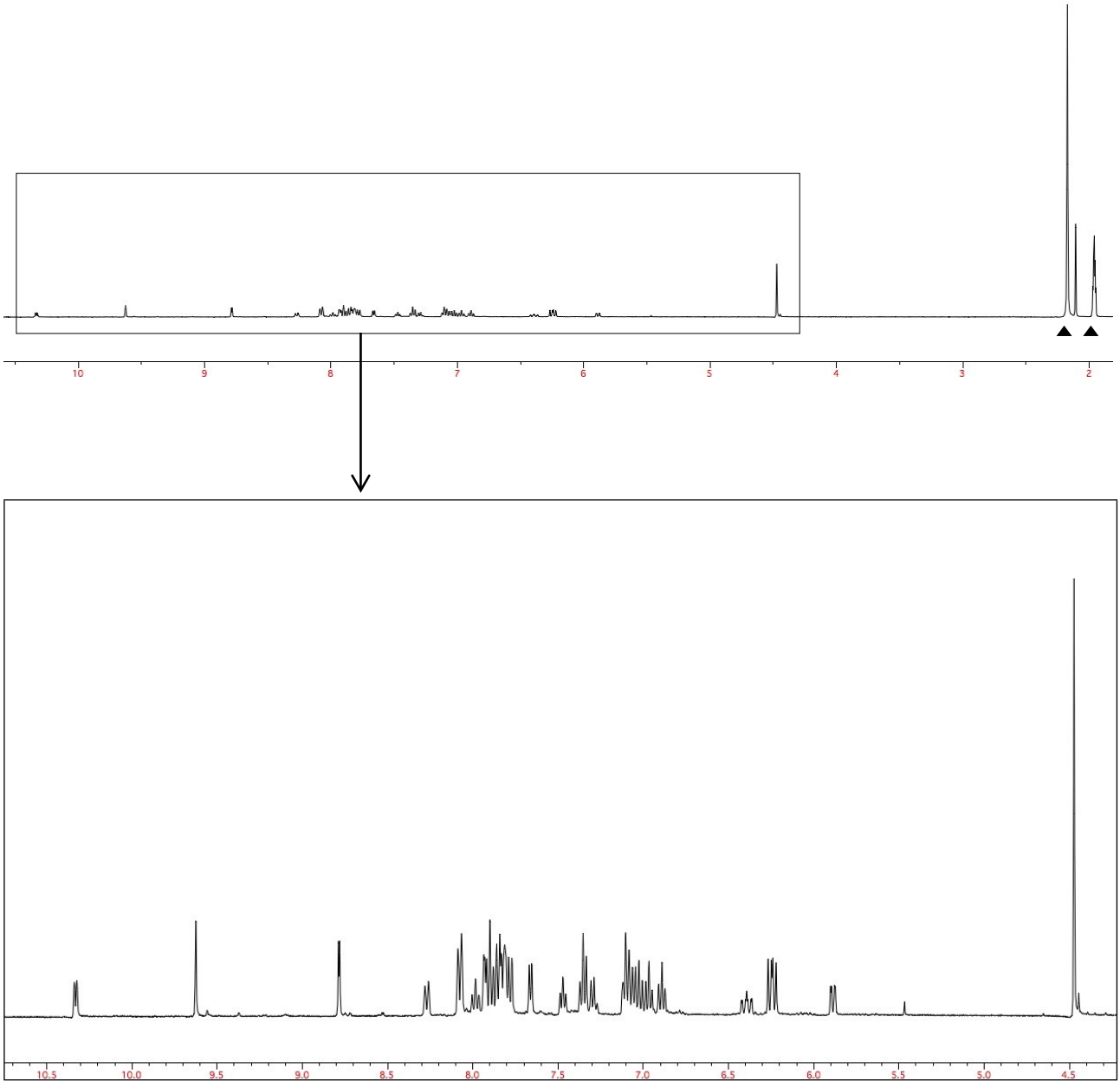

▲= ^{1}H signals of residual of non deuterated CD_3CN and water.

Figure S15: ESI-MS spectrum (negative ions region) of **$[Ir(Tph)_2]^-$**, $[M]^-$ = 791 (*m/z*).

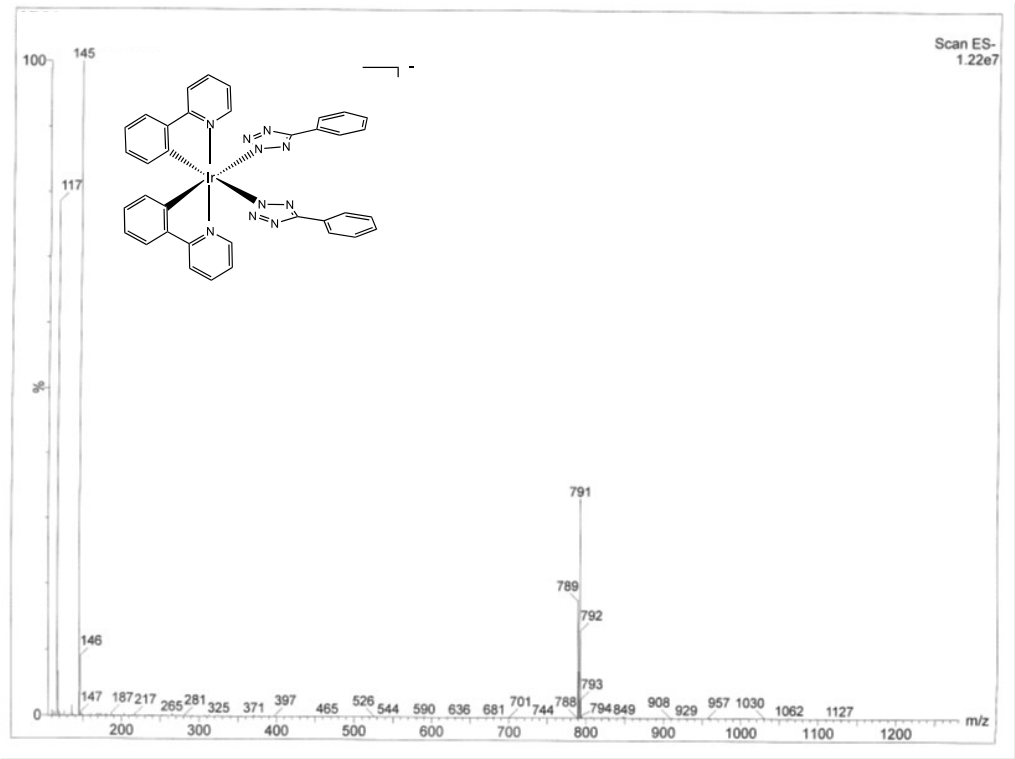

Figure S16: ESI-MS spectrum (negative ions region) of **$[F_2Ir(Tph)_2]^-$**, $[M]^-$ = 863 (*m/z*).

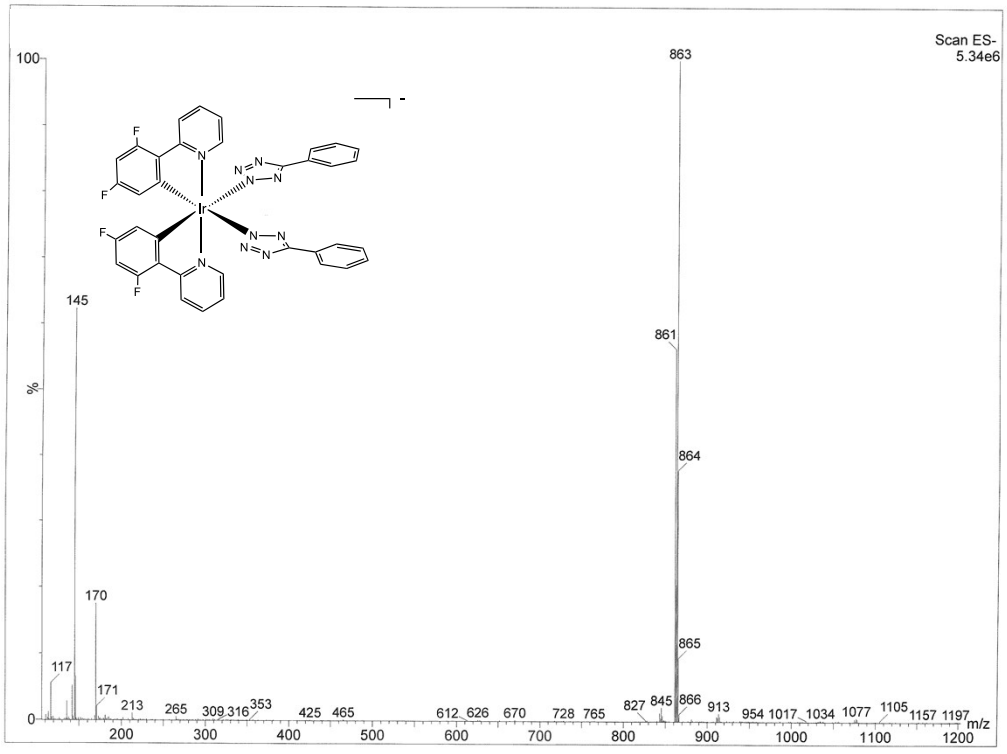

Figure S17: ESI-MS spectrum (negative ions region) of **$[Ir(TphCN)_2]^-$**, $[M]^-$ = 841 (*m/z*).

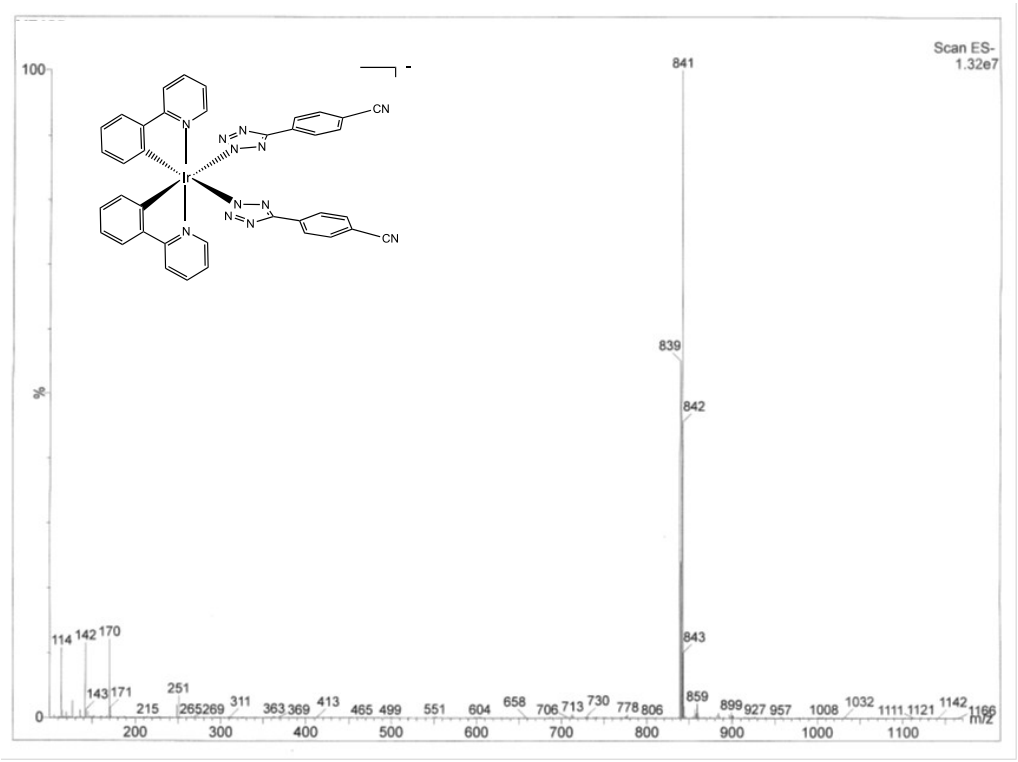

Figure S18: ESI-MS spectrum (negative ions region) of **$[F_2Ir(TphCN)_2]^-$**, $[M]^-$ = 913 (*m/z*).

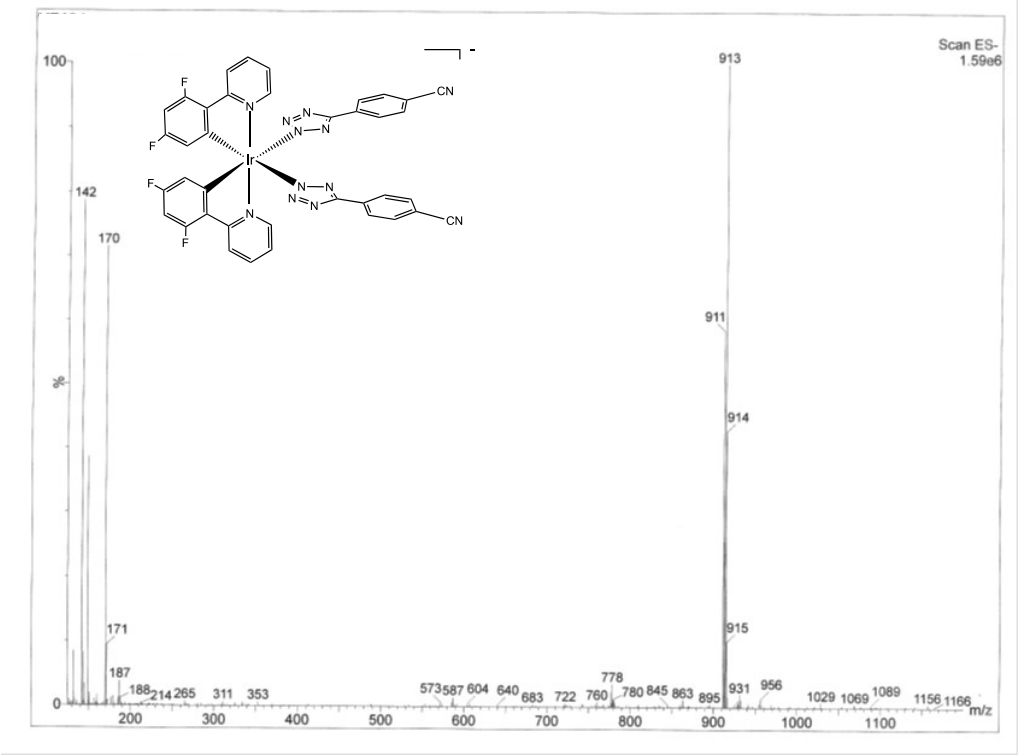

Figure S19: ESI-MS spectrum (positive ions region) of **[IrTPYZ-Me]$^+$**, $[M]^+$ = 663 (*m/z*).

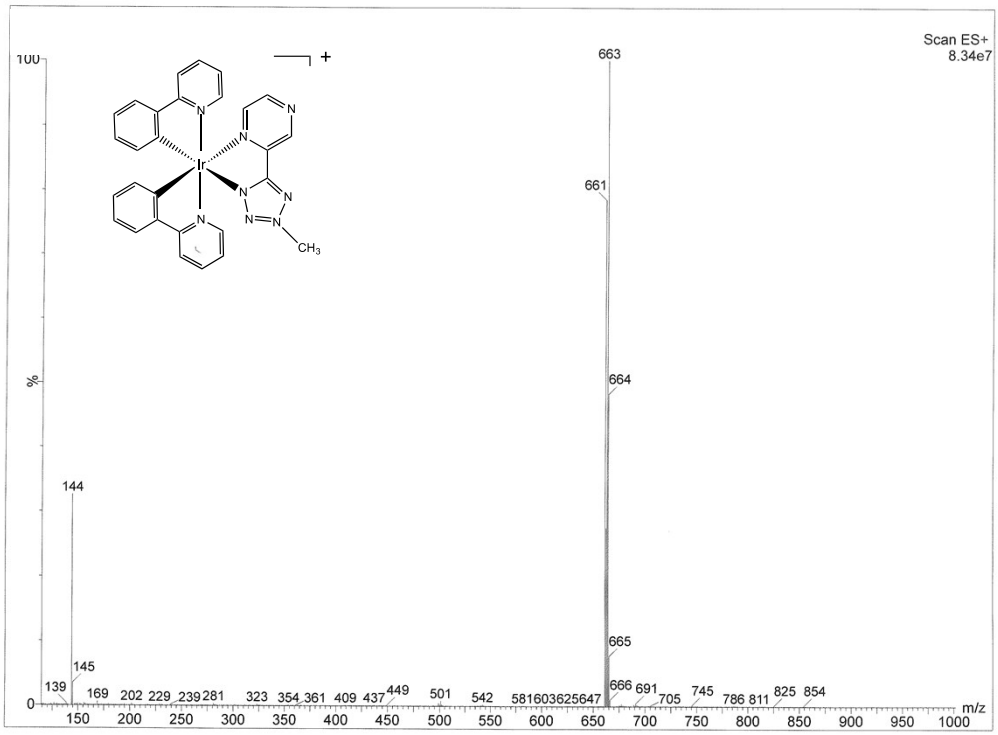

Anionic Ir(III) tetrazolate complexes photophysical characterization

Figure S20: Left - Absorption profile **[Ir(Tph)$_2$]$^-$**, Right – Excitation profile **[Ir(Tph)$_2$]$^-$** λ_{emi} = 492 nm; CH_2Cl_2, r.t.

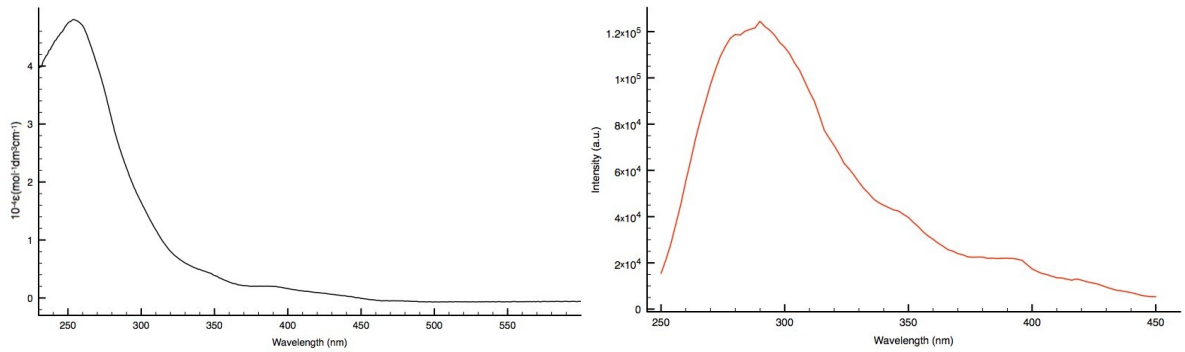

Figure S21: Emission spectra **[Ir(Tph)$_2$]$^-$**, 298K (black line), 77K (blue line), CH_2Cl_2.

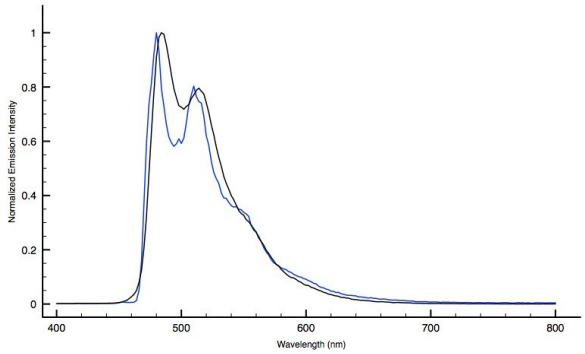

Figure S22: Emission spectra **[Ir(Tph)$_2$]$^-$** 298K oxygenated solution (black line), 298K deoxygenated solution (blue line), CH_2Cl_2.

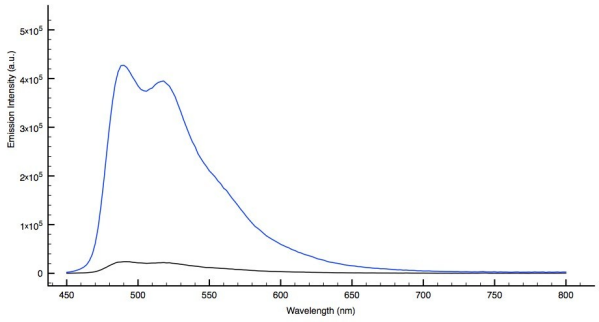

Figure S23: Emission spectra **[Ir(Tph)$_2$]$^-$**, neat solid r.t.

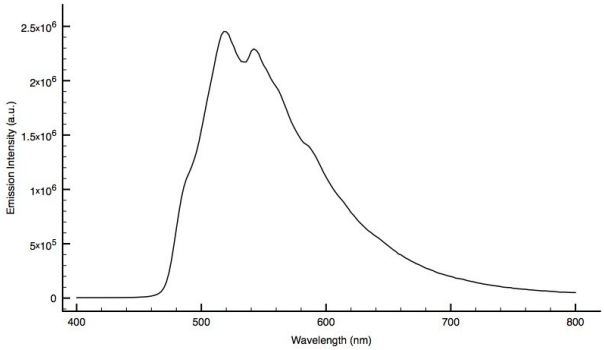

Emission Neat Solid r.t.	
λ_{em} (nm)	τ (μs)
520	0.168
542	0.234

Figure S24: Left - Absorption profile **$[F_2Ir(Tph)_2]^-$**, Right – Excitation profile **$[F_2Ir(Tph)_2]^-$** λ_{emi} = 462 nm; CH_2Cl_2, r.t.

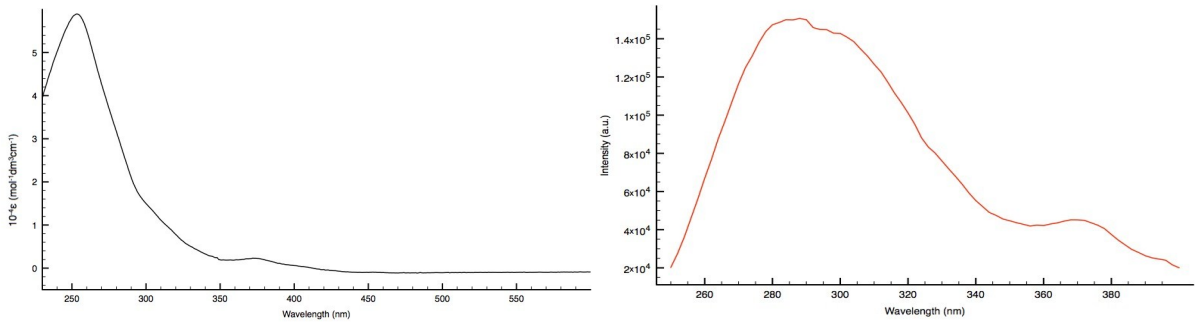

Figure S25: Emission spectra **$[F_2Ir(Tph)_2]^-$**, 298K (black line), 77K (blue line), CH_2Cl_2.

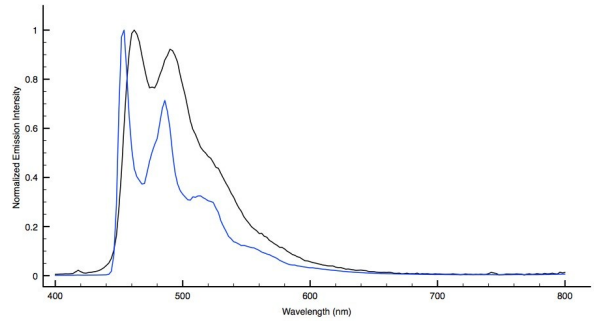

Figure S26: Emission spectra **$[F_2Ir(Tph)_2]^-$** 298K oxygenated solution (black line), 298K deoxygenated solution (blue line), CH_2Cl_2.

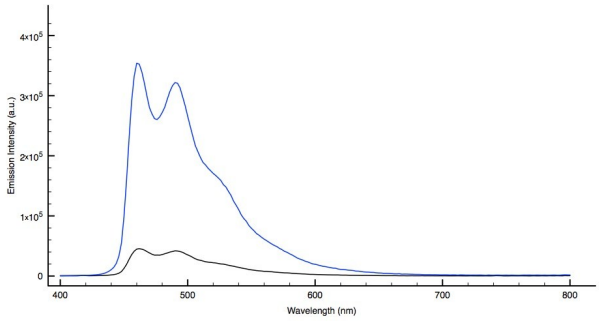

Figure S27: Emission spectra **$[F_2Ir(Tph)_2]^-$**, neat solid r.t.

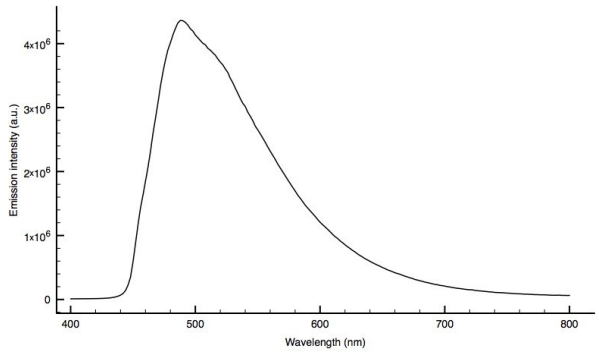

Emission Neat solid r.t.	
λ_{em} (nm)	τ (µs)
488	0.295

Figure S28: Left - Absorption profile **[Ir(TphCN)$_2$]$^-$**, Right – Excitation profile **[Ir(TphCN)$_2$]$^-$** λ_{emi} = 490 nm; CH_2Cl_2, r.t.

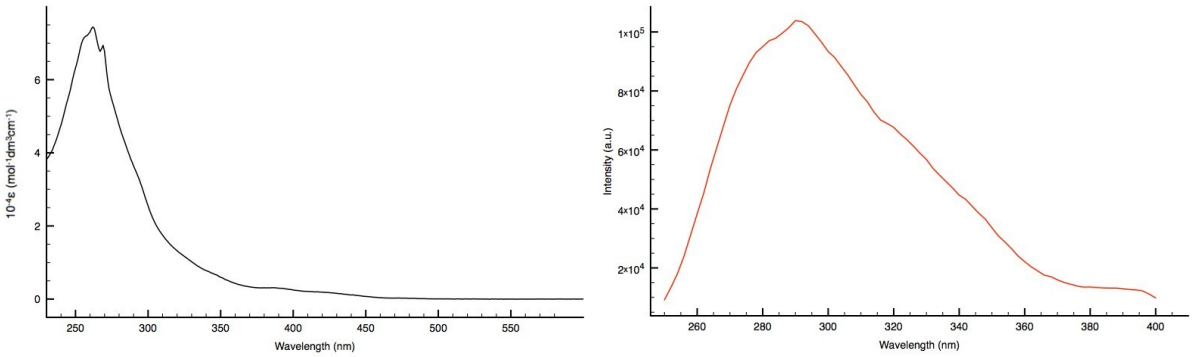

Figure S29: Emission spectra **[Ir(TphCN)$_2$]$^-$**, 298K (black line), 77K (blue line), CH_2Cl_2.

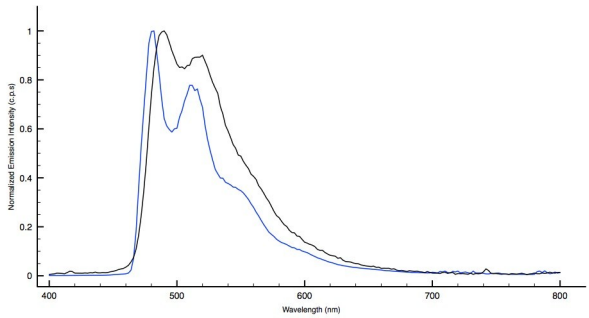

Figure S30: Emission spectra **[Ir(TphCN)$_2$]$^-$** 298K oxygenated solution (black line), 298K deoxygenated solution (blue line), CH_2Cl_2.

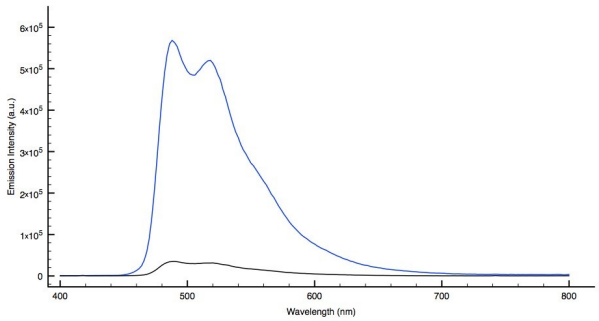

Figure S31: Emission spectra **[Ir(TphCN)$_2$]$^-$**, neat solid r.t.

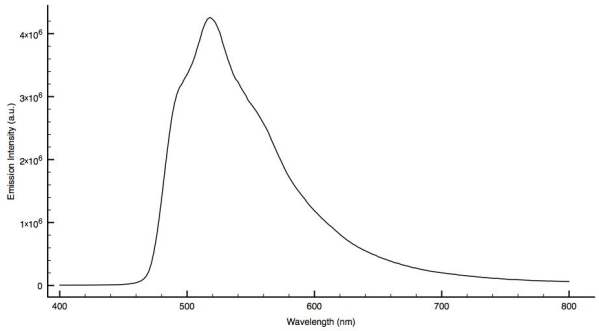

Emission Neat Solid r.t.	
λ_{em} (nm)	τ (μs)
518	0.383

Figure S32: Left - Absorption profile **$[F_2Ir(Tph)_2]^-$**, Right – Excitation profile **$[F_2Ir(Tph)_2]^-$** λ_{emi} = 462 nm; CH_2Cl_2, r.t.

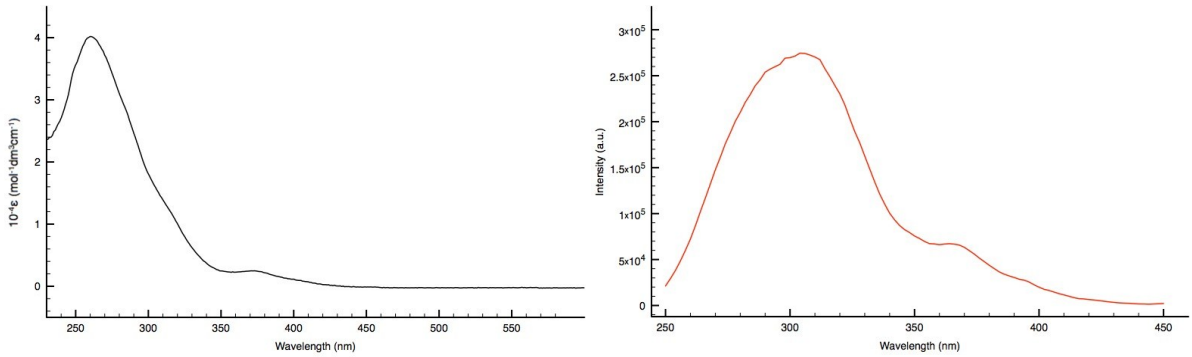

Figure S33: Emission spectra **$[F_2Ir(TphCN)_2]^-$**, 298K (black line), 77K (blue line), CH_2Cl_2

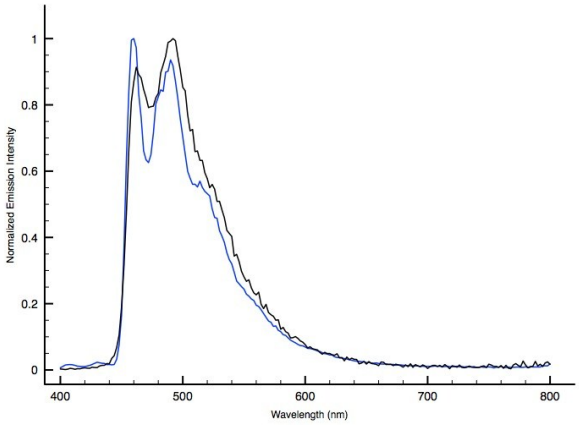

Figure S34: Emission spectra **$[F_2Ir(TphCN)_2]^-$** 298K oxygenated solution (black line), 298K deoxygenated solution (blue line), CH_2Cl_2.

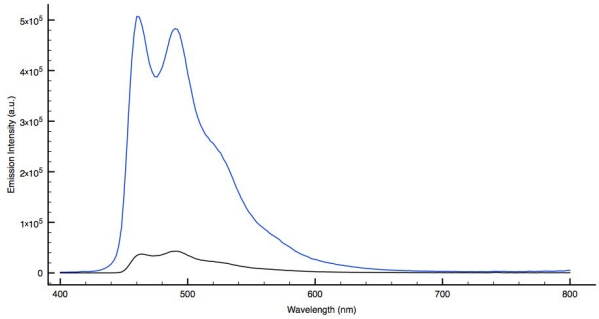

Figure S35: Emission spectra **$[F_2Ir(TphCN)_2]^-$**, neat solid r.t.

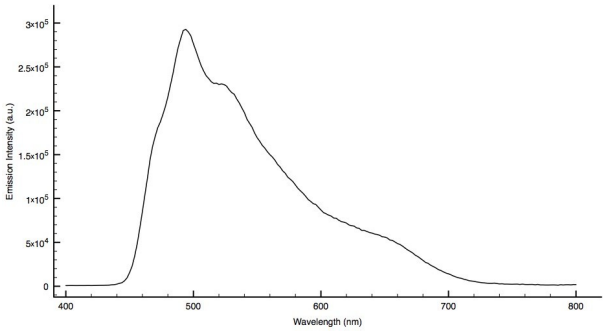

Emission Neat Solid r.t.	
λ_{em} (nm)	τ (μs)
494	
524	0.118
630	

Figure S36: Normalized Emission Profiles, 298K oxygenated solution of **$[F_2Ir(Tph)_2]^-$** (blue line), **$[Ir(Tph)_2]^-$** (red line), CH_2Cl_2.

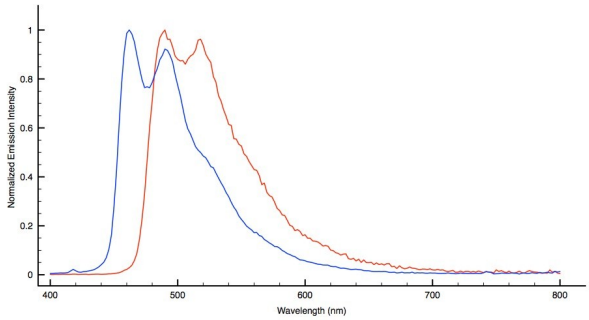

Figure S37: Normalized Emission Profiles, 298K oxygenated solution of **$[F_2Ir(TphCN)_2]^-$** (blue line), **$[Ir(TphCN)_2]^-$** (red line), CH_2Cl_2.

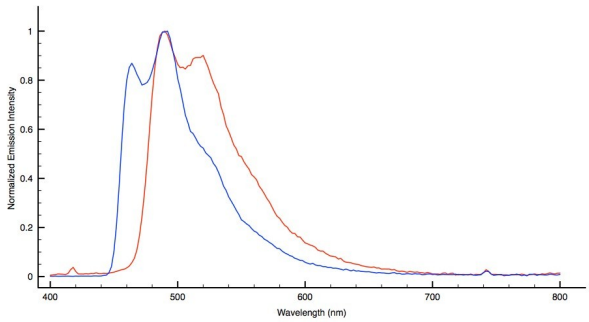

Cationic Ir(III) tetrazolate complex photophysical characterization

Figure S38: Left - Absorption profile **[IrTPYZ-Me]$^+$**, Right – Excitation profile **[IrTPYZ-Me]$^+$**, λ_{emi} = 680 nm; CH_2Cl_2, r.t.

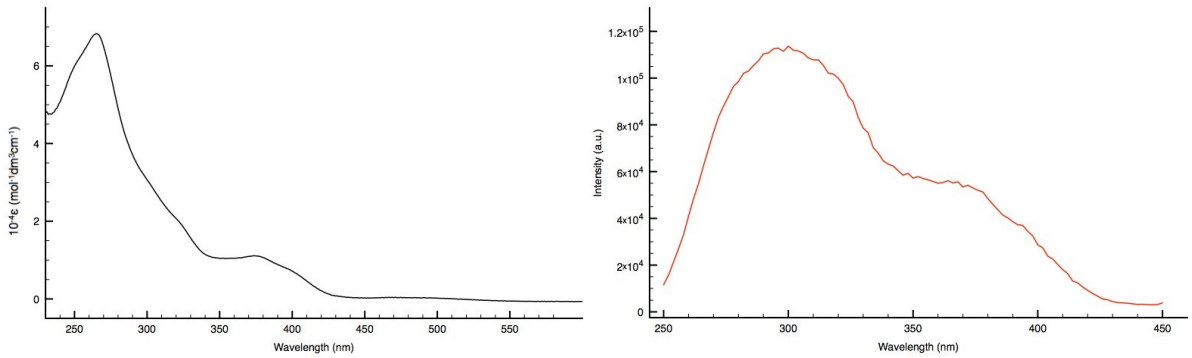

Figure S39: Emission spectra **[IrTPYZ-Me]$^+$**, 298K (black line), 77K (blue line), CH_2Cl_2.

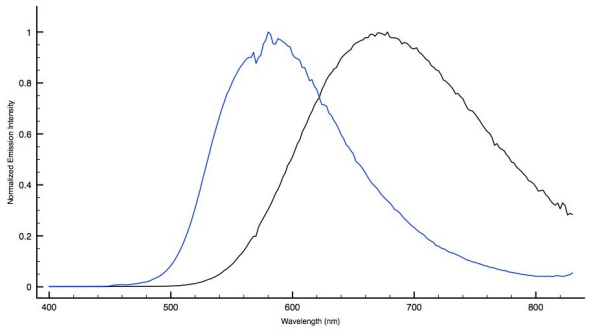

Figure S40: Emission spectra **[IrTPYZ-Me]$^+$** 298K oxygenated solution (black line), 298K deoxygenated solution (blue line), CH_2Cl_2.

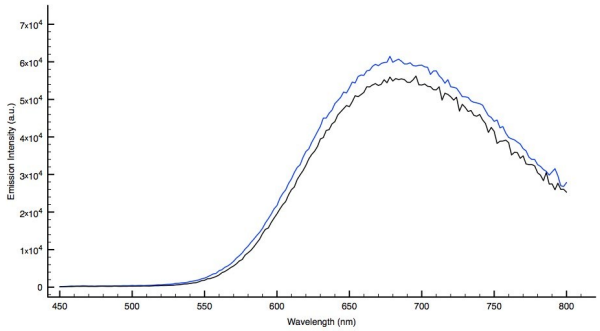

Figure S41: Emission spectra **[IrTPYZ-Me]**$^{+}$, neat solid r.t.

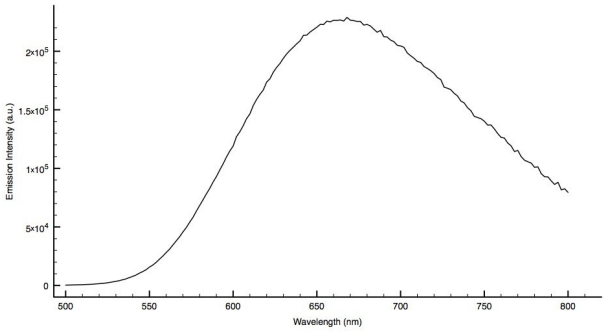

Emission Neat Solid r.t.	
λ_{em} (nm)	τ (μs)
664	0.114 (47) 0.264 (53)

Ir(III) Soft Salts photophysical characterization

Table S2: Photophysical data for **SS1**

Absorption		*Emission 298K*					*Emission 77K*		*Emission Neat Solid r.t.*		*C.I.E*	
Complex (Solvent: CH_2Cl_2)	λ_{abs} (nm): ($10^{-4}\varepsilon$)($M^{-1}cm^{-1}$)	λ_{em} (nm)	τ_{air} (μs)	τ_{Ar} (μs)	φ_{air} (%)	φ_{Ar} (%)	λ_{em} (nm)	τ_{air} (μs)	λ_{em} (nm)	τ (μs)	*air*	*Under Ar*
SS1	261(4.93), 314(1.50), 377(0.39)	460 490 680	0.156 0.152 0.099	1.188 1.116 0.105	2.82	7,02	454 484 574	3.750 3.930 4.570	660	0.239	X=0.3288 Y=0.3284	X=0.2033 Y=0.3202

Figure S42: Left - Absorption profile **SS1**; Right – Normalized Excitation profiles **SS1** λ_{emi} = 460 nm (black trace), 490 nm (blue trace) 680 nm (red trace), CH_2Cl_2, r.t.

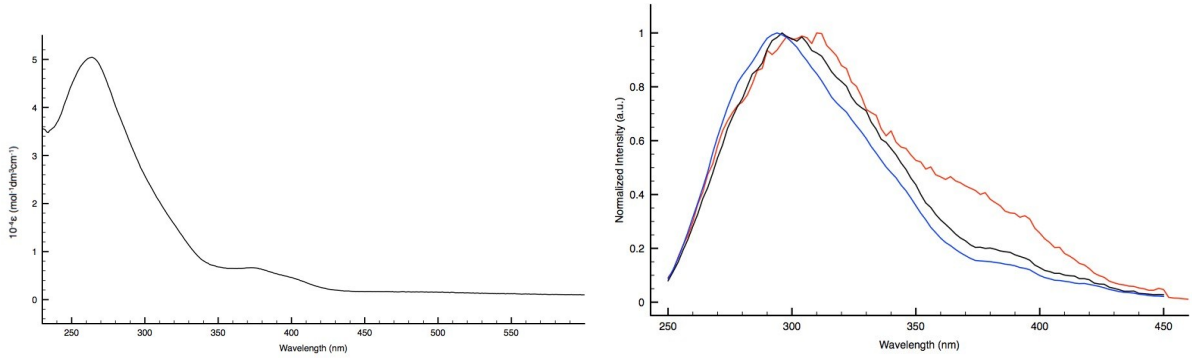

Figure S43: Absorption profile of **SS1** (black line), **$[F_2Ir(TphCN)_2]^-$** (blue line), **[IrTPYZ-Me]$^+$** (red line), CH_2Cl_2.

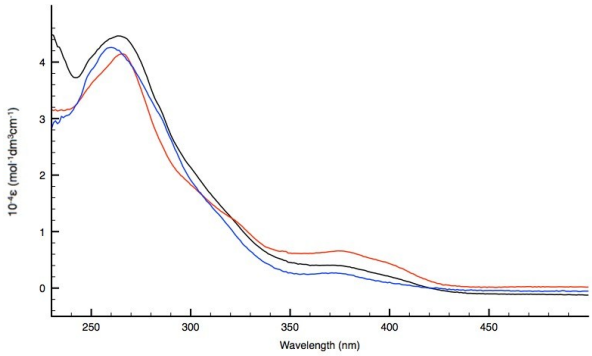

Figure S44: Emission spectra of **SS1** oxygenated solution (red line), deoxygenated solution (blue line), 298K, CH_2Cl_2.

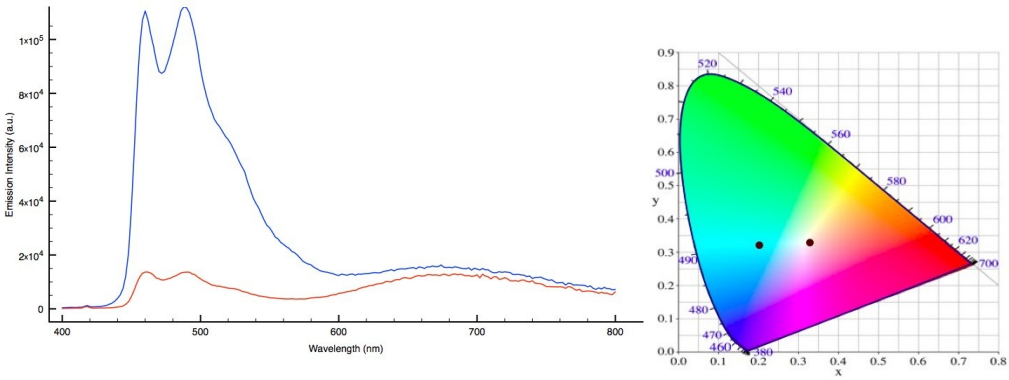

Figure S45: Emission spectra of **SS1**, 10^{-5}M (red trace), 10^{-6}M (blue trace) CH_2Cl_2, r.t.

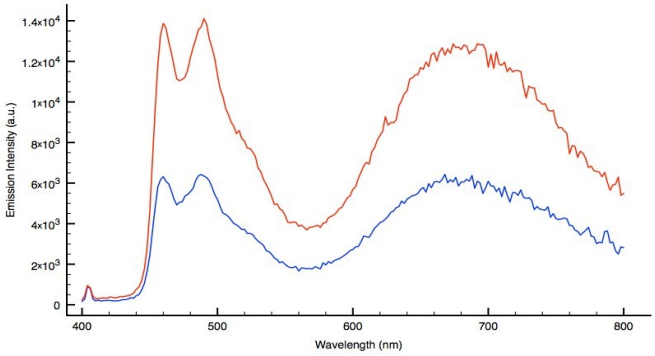

Figure S46: Emission spectra of **SS1**, 77K, CH_2Cl_2.

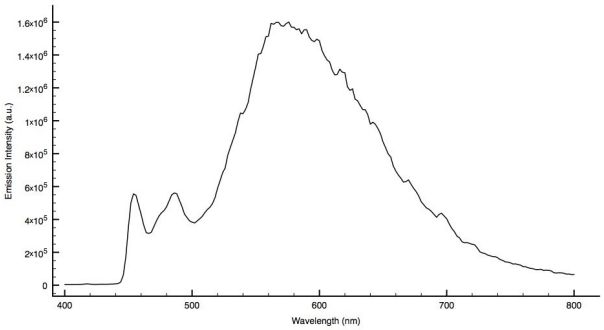

Figure S47: Emission spectra of **SS1** (black line), **[F_2Ir(TphCN)$_2$]**$^-$ (blue line), [**IrTPYZ-Me**]$^+$ (red line), neat solid r.t.

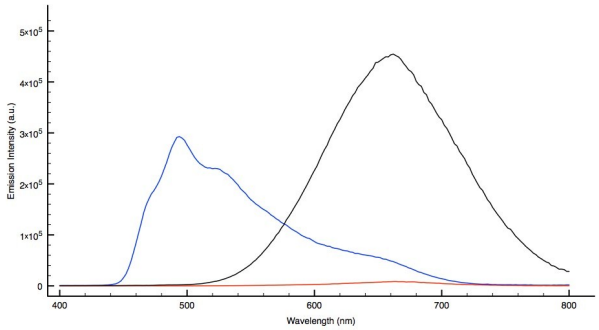

Table S3: Photophysical data for **SS2**

Absorption		*Emission 298K*					*Emission 77K*		*Emission Neat Solid r.t.*		*C.I.E*	
Complex (CH_2Cl_2)	λ_{abs} (nm): ($10^{-4}\varepsilon$)($M^{-1}cm^{-1}$)	λ_{em} (nm)	τ_{air} (μs)	τ_{Ar} (μs)	φ_{air} (%)	φ_{Ar} (%)	λ_{em} (nm)	τ (μs)	λ_{em} (nm)	τ (μs)	*air*	*Under Ar*
SS2	263(7.09), 343(1.18), 385(0.69)	486 518 664	0.102 0.100 0.110	0.659 0.654 0.137	3.41	14.83	480 574	1.076 2.452	730	0.100	X=0.4483 Y=0.4461	X=0.2825 Y=0.5171

Figure S48: Left - Absorption profile **SS2**; Right – Normalized Excitation profiles **SS2** λ_{emi} = 486 nm (black trace), 518 nm (blue trace) 664 nm (red trace), CH_2Cl_2, r.t.

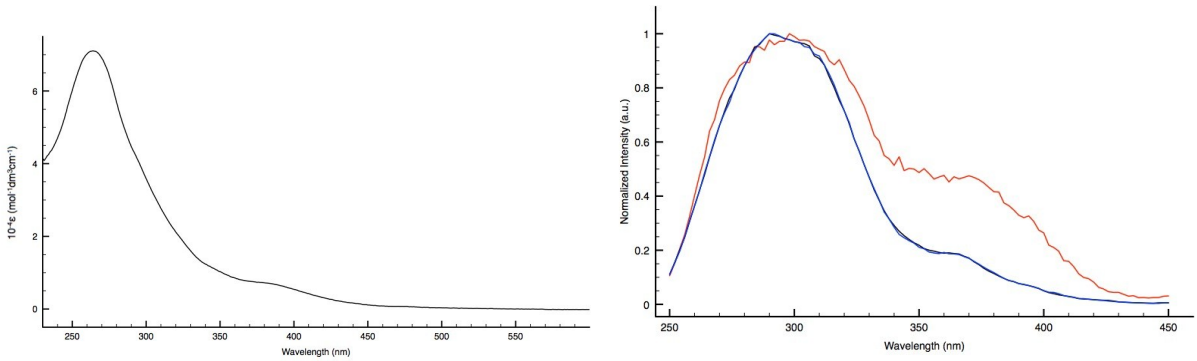

Figure S49: Absorption profile of **SS2** (black line), **[Ir(TphCN)$_2$]$^-$** (blue line), [**IrTPYZ-Me**]$^+$ (red line), CH_2Cl_2, r.t.

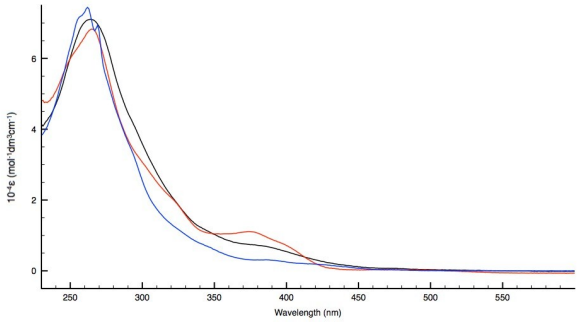

Figure S50: Emission spectra of **SS2** oxygenated solution (red line), deoxygenated solution (blue line), 298K, CH_2Cl_2, r.t.

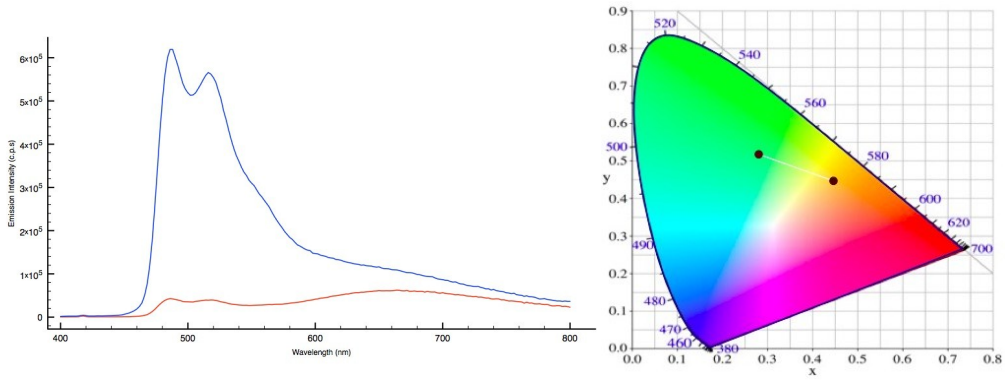

Figure S51: Emission profile of **SS2**, 10^{-5}M (red trace), 10^{-6}M (blue trace) CH_2Cl_2, r.t.

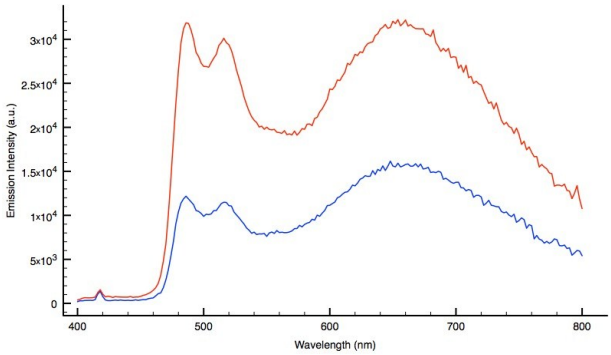

Figure S52: Emission spectra of **SS2**, 77K, CH_2Cl_2.

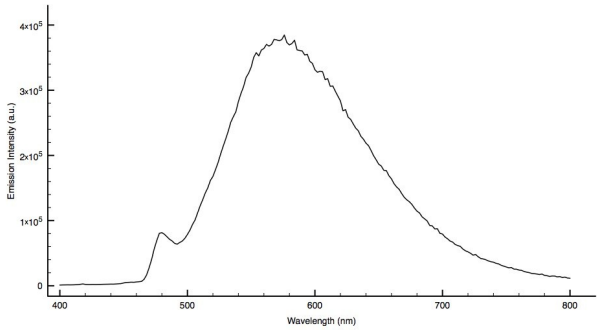

Figure S53: Emission spectra of **SS2**, neat solid r.t.

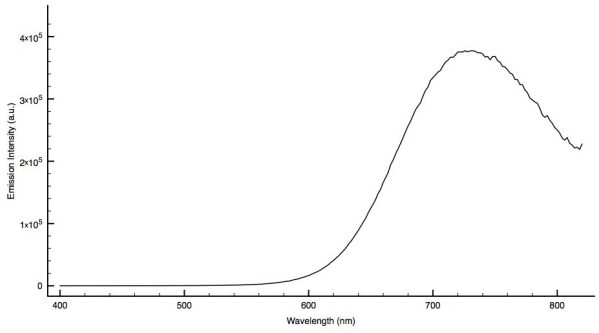

Figure S54: Emission spectra of **SS2** (black line), **[Ir(TphCN)$_2$]$^-$** (blue line), [**IrTPYZ-Me**]$^+$ (red line), neat solid r.t.

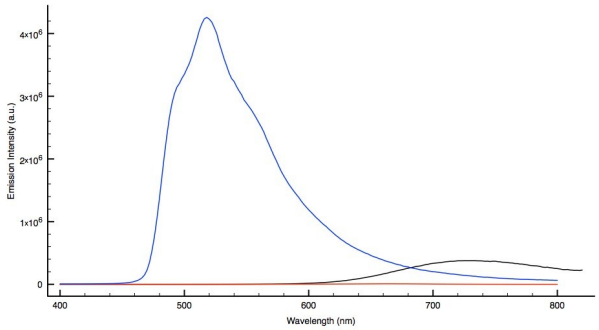

Table S4: Photophysical data for **SS3**

Absorption		*Emission 298K*					*Emission 77K*		*Emission Neat Solid r.t.*		*C.I.E*	
Complex (Solvent: CH_2Cl_2)	λ_{abs} (nm): ($10^{-4}\varepsilon$)($M^{-1}cm^{-1}$)	λ_{em} (nm)	τ_{air} (µs)	τ_{Ar} (µs)	φ_{air} (%)	φ_{Ar} (%)	λ_{em} (nm)	τ (µs)	λ_{em} (nm)	τ (µs)	*air*	*Under Ar*
SS3	262(5.19) 320(1.49) 381(0.63)	486 518 680	0.121 0.120 0.098	1.461 1.441 0.105	3.56	12.3	480 574 510	3.130 3.160 3.270	712	0.105	X=0.4634 Y=0.4308	X=0.273 Y=0.5102

Figure S55: Left - Absorption profile **SS3**; Right – Normalized Excitation profiles **SS3** λ_{emi} = 486 nm (black trace), 518 nm (blue trace) 680 nm (red trace), CH_2Cl_2, r.t.

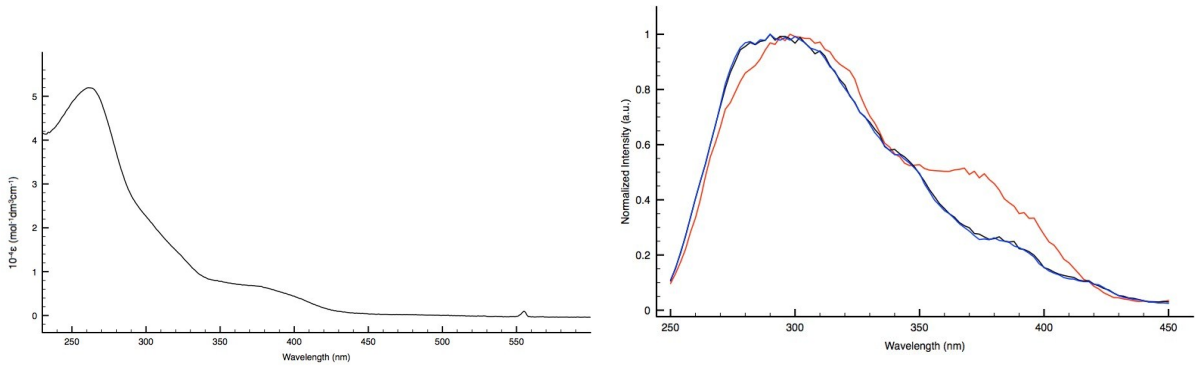

Figure S56: Absorption profile of **SS3** (black line), **[Ir(Tph)$_2$]$^-$** (blue line), [**IrTPYZ-Me**]$^+$ (red line), CH_2Cl_2, r.t.

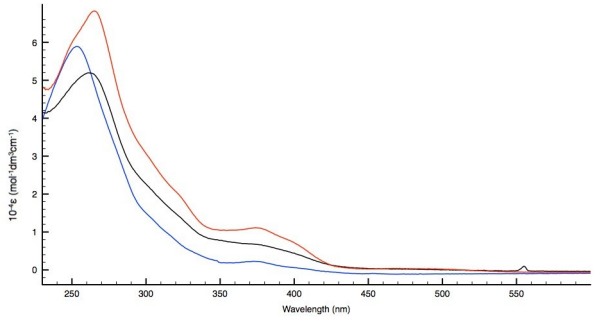

Figure S57: Emission spectra of **SS3** oxygenated solution (red line), deoxygenated solution (blue line), 298K, CH_2Cl_2, r.t.

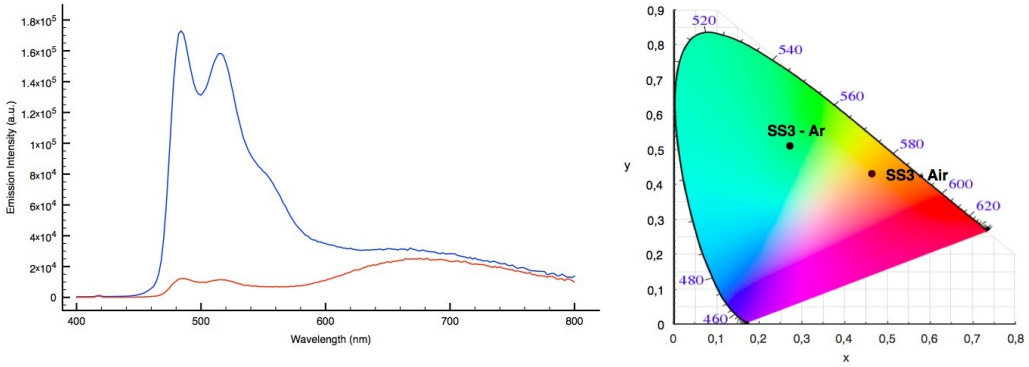

Figure S58: Emission spectra of **SS3**, 10^{-5}M (red trace), 10^{-6}M (blue trace) CH_2Cl_2, r.t.

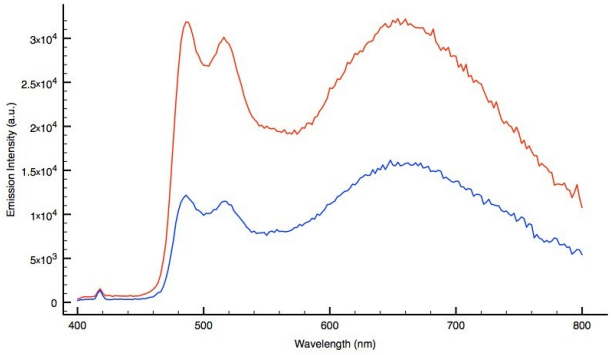

Figure S59: Emission spectra of **SS3** (black line), **$[Ir(Tph)_2]^-$** (blue line), [**IrTPYZ-Me**]$^+$ (red line), neat solid r.t.

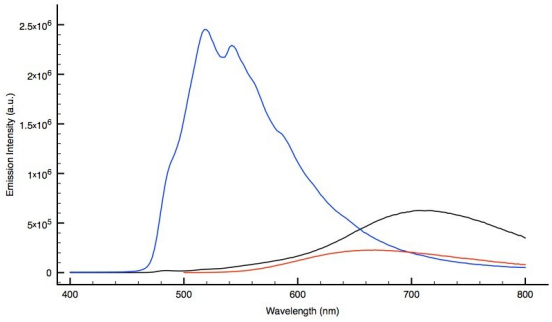

Table S5: Photophysical data for **SS4**

Absorption		*Emission 298K*					*Emission 77K*		*Emission Neat Solid r.t.*		*C.I.E*	
Complex (Solvent: CH_2Cl_2)	λ_{abs} (nm): ($10^{-4}\varepsilon$)($M^{-1}cm^{-1}$)	λ_{em} (nm)	τ_{air} (μs)	τ_{Ar} (μs)	φ_{air} (%)	φ_{Ar} (%)	λ_{em} (nm)	τ (μs)	λ_{em} (nm)	τ (μs)	*air*	*Under Ar*
SS4	255(3.60) 317(0.95) 377(0.43)	462 490 680	0.190 0.198 0.094	1.280 1.220 0.103	3.02	16.9	454 488 578	2.280 2.800 3.066	654	0.304	X=0.308 Y=0.3298	X=0.1972 Y=0.3277

Figure S60: Left - Absorption profile **SS4**; Right – Normalized Excitation profiles **SS4** λ_{emi} = 462 nm (black trace), 490 nm (blue trace) 680 nm (red trace), CH_2Cl_2, r.t.

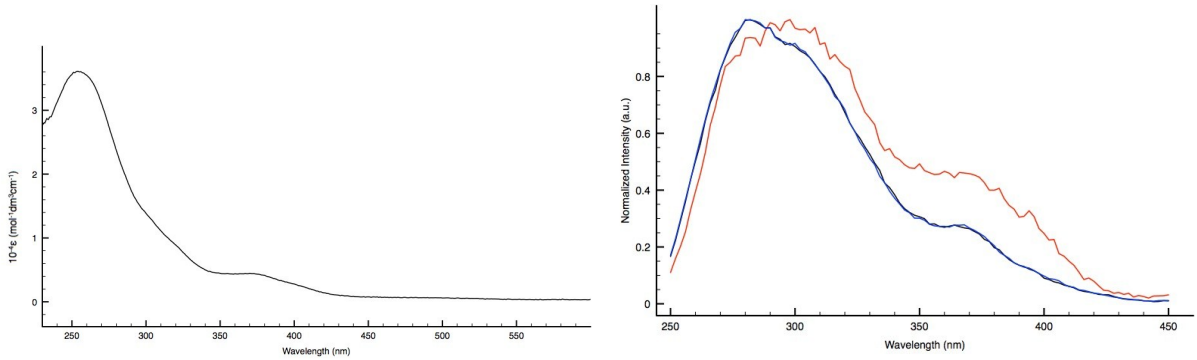

Figure S61: Absorption profile of **SS4** (black line), **$[F_2Ir(Tph)_2]^-$** (blue line), **[IrTPYZ-Me]$^+$** (red line), CH_2Cl_2, r.t.

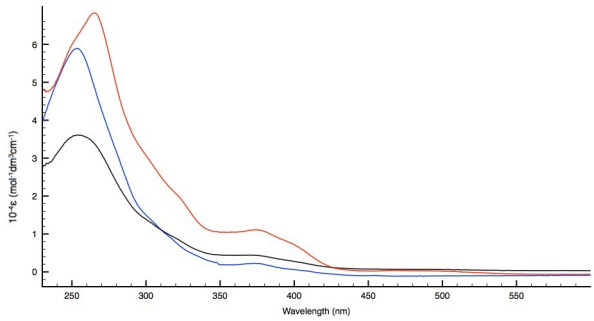

Figure S62: Emission spectra of **SS4** oxygenated solution (red line), deoxygenated solution (blue line), 298K, CH_2Cl_2, r.t.

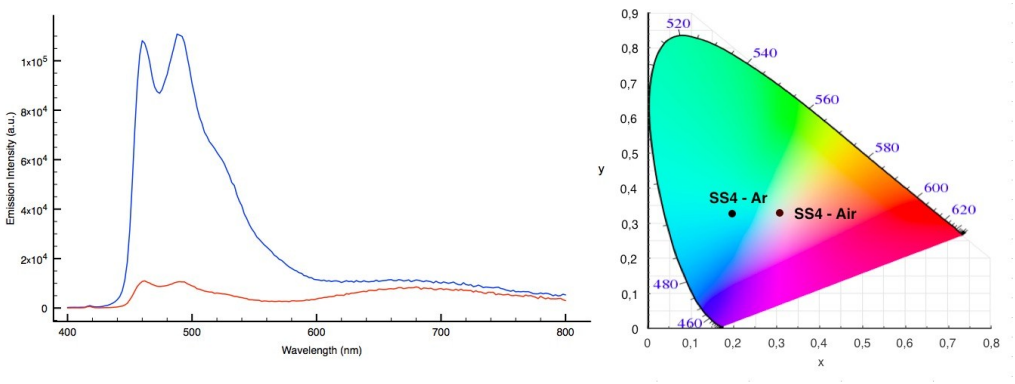

Figure S63: Emission spectra of **SS4**, 10^{-5}M (red trace), 10^{-6}M (blue trace) CH_2Cl_2, r.t.

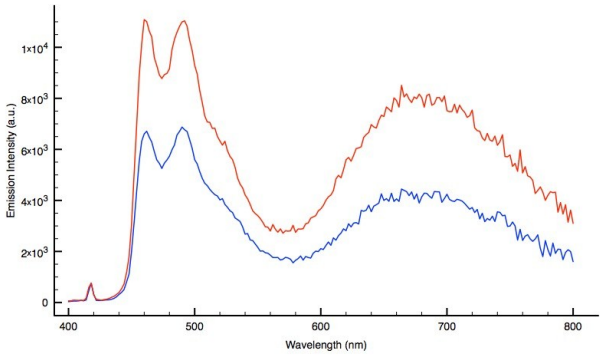

Figure S64: Emission spectra of **SS4** (black line), **$[F_2Ir(Tph)_2]^-$** (blue line), [**IrTPYZ-Me**]$^+$ (red line), neat solid r.t.

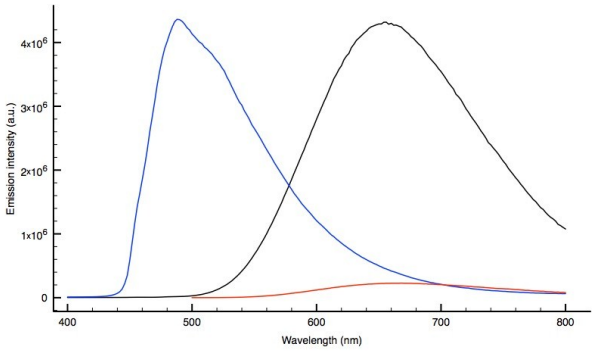

Table S6: Stern Volmer data summary for **SS3**.

time (min)[a]	I0/I[b]	τ0/τ[c]
0[d]	1	1
2	1.073	
4	1.225	
6	1.679	
8	1.947	
10	2.148	2.70
12	2.293	
14	2.426	
18	2.466	
20	2.622	4.35
22	2.607	
24	2.716	
26	2.774	
28	2.837	
30	2.880	5.38
32	2.935	
34	2.959	
36	2.978	
38	3.014	
40	3.031	6.06
42	3.054	
44	3.068	
46	3.086	
48	3.057	
50	3.051	6.37
52	3.068	
54	3.054	
56	3.103	
58	3.109	
60	3.121	
62	3.097	
64	3.145	
66	3.157	
68	3.161	
70	3.170	
72	3.183	
78	3.097	

a = Sum of the acquisition time for the emission spectrum (dwell time = 0.250. 1 minute for each spectrum from 400 to 800 nm. λ_{exc} = 370 nm) and waiting time between each scan (1 minute) for 37 total scans.

b = integral of the emission profile of the degassed sample after the solution was bubbled for 10 minutes under Ar atmosphere using a septa-sealed quartz cell (**I0**) over the integral of the emission profile after (minutes) of air re-equilibration of the sample by the removal of the septum (**I**).

c = lifetime value of the degassed sample after the solution was bubbled for 10 minutes under Ar atmosphere using a septa-sealed quartz cell (**τ0**) over lifetime value after (minutes) of air re-equilibration of the sample by the removal of the septum (**τ**). During the acquisition of each decay time (periods of 2 minutes) the quartz cuvette was sealed in order to prevent uncontrolled air contamination of the sample. Emission lifetimes were determined using pulsed picosecond LED as the excitation source (369 nm) at λ_{max} = 486 nm.

d = sample under Ar atmosphere, closed vessel.

Figure S65: Multiple Emission Scans of **SS3** from deoxygenated to air equilibrated solution, 37 scans recorded at 2 minutes intervals, CH_2Cl_2, r.t.

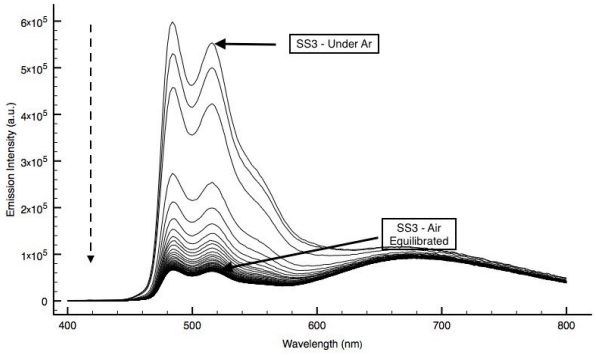

Figure S66: Decay times of **SS3** (at λ_{max} = 486 nm) recorded during the Stern Volmer analysis at 10 minutes intervals, CH_2Cl_2, r.t.

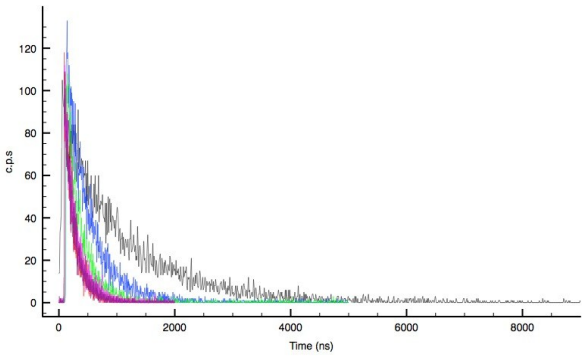

Figure S67: Stern Volmer Plot of **SS3**.

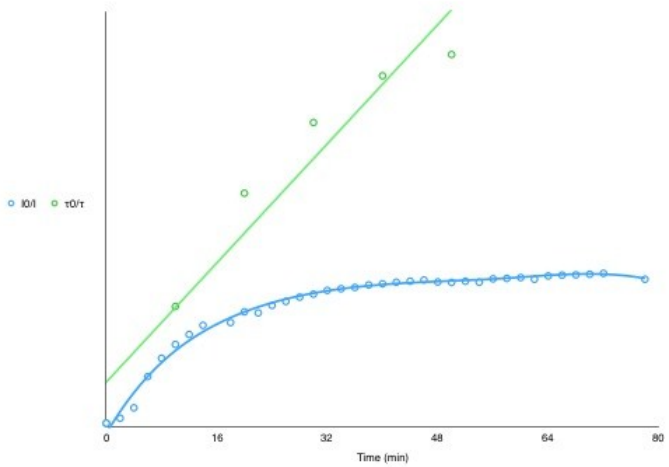

Table S7: Stern Volmer data summary for **SS4**.

time (min)[a]	I0/I[b]	τ0/τ[c]
0[d]	1	1
2	1.06	
4	1.44	
6	1.68	
8	1.91	
10	2.12	2.27
12	2.30	
14	2.48	
18	2.65	
20	2.80	4.45
22	2.92	
24	3.03	
26	3.14	
28	3.24	
30	3.31	4.97
32	3.40	
34	3.45	
36	3.56	
38	3.57	
40	3.61	5.87
42	3.65	
44	3.69	
46	3.72	
48	3.75	
50	3.79	6.11
52	3.80	
54	3.83	
56	3.82	
58	3.86	
60	3.85	
62	3.86	
64	3.84	
66	3.88	
68	3.91	
70	3.87	
72	3.91	
78	3.85	

a = Sum of the acquisition time for the emission spectrum (dwell time = 0.250. 1 minute for each spectrum from 400 to 800 nm. λ_{exc} = 370 nm) and waiting time between each scan (1 minute) for 37 total scans.

b = integral of the emission profile of the degassed sample after the solution was bubbled for 10 minutes under Ar atmosphere using a septa-sealed quartz cell (**I0**) over the integral of the emission profile after (minutes) of air re-equilibration of the sample by the removal of the septum (**I**).

c = lifetime value of the degassed sample after the solution was bubbled for 10 minutes under Ar atmosphere using a septa-sealed quartz cell (**τ0**) over lifetime value after (minutes) of air re-equilibration of the sample by the removal of the septum (**τ**). During the acquisition of each decay time (periods of 2 minutes) the quartz cuvette was sealed in order to prevent uncontrolled air contamination of the sample. Emission lifetimes were determined using pulsed picosecond LED as the excitation source (369 nm) at λ_{max} = 460 nm.

d = sample under Ar atmosphere, closed vessel.

Figure S67: Multiple Emission Scans of **SS4** from deoxygenated to air equilibrated solution, 37 scans recorded at 2 minutes intervals, CH_2Cl_2, r.t.

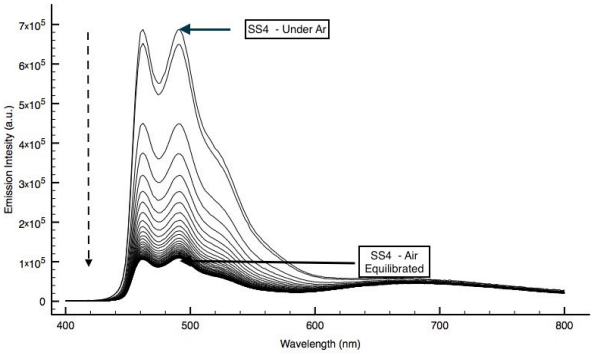

Figure S68: Decay times of **SS4** (at λ_{max} = 460 nm) recorded during the Stern Volmer analysis at 10 minutes intervals, CH_2Cl_2, r.t.

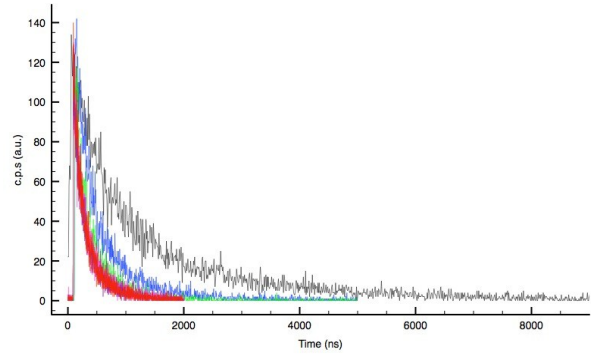

Figure S69: Stern Volmer Plot of **SS4**.

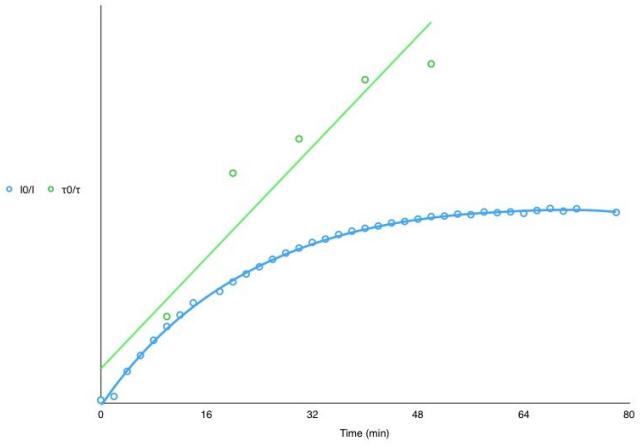

The Stern-Volmer plot for **SS3** and **SS4** are observed to curve downwards towards the *x*- axis (**I0**/**I** vs Time, blue trace), which is characteristic of two populations of fluorophore[viii] (anion and cation contribution to the ion pair), one of which is less sensitive to the quencher (O_2).

Figure S70: $[F_2Ir(TphCN)_2]^-$ 10^{-5}M, air equilibrated (left) **$[Ir(TphCN)_2]^-$** 10^{-5}M air equilibrated (right), CH_2Cl_2, r.t; λ_{exc}= 365 nm.

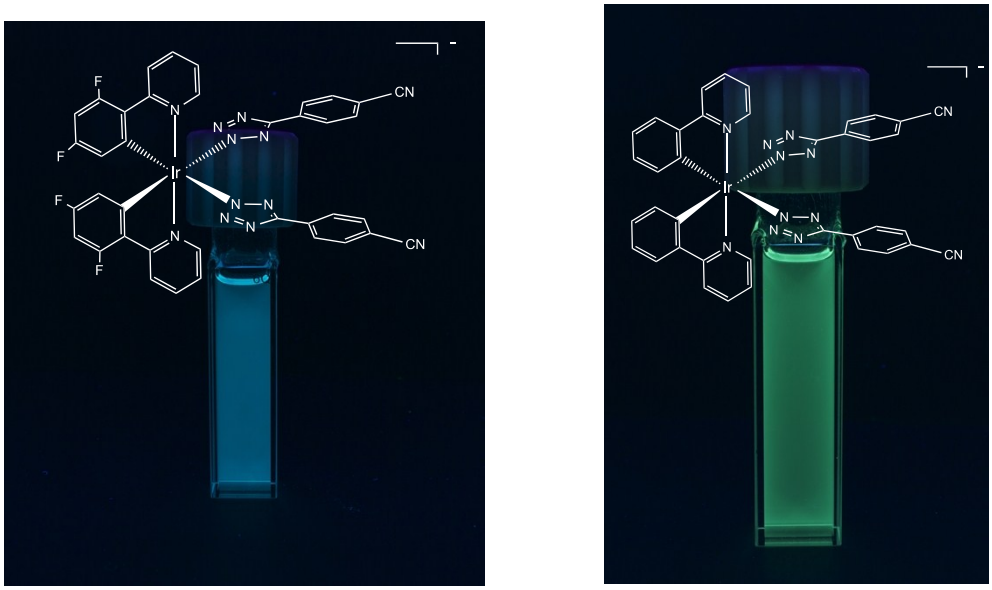

Figure S71: $[IrTPYZ\text{-}Me]^+$ 10^{-5}M, air equilibrated solution, CH_2Cl_2, r.t; λ_{exc}= 365 nm.

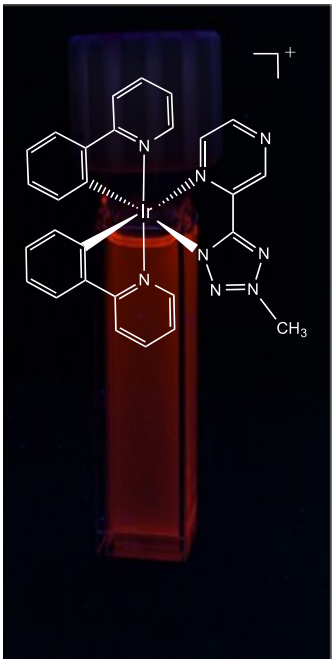

Figure S72: **SS1**, 10^{-5}M, air equilibrated (left) **SS1**, 10^{-5}M, deoxygenated solution (right), CH_2Cl_2, r.t; λ_{exc}= 365 nm.

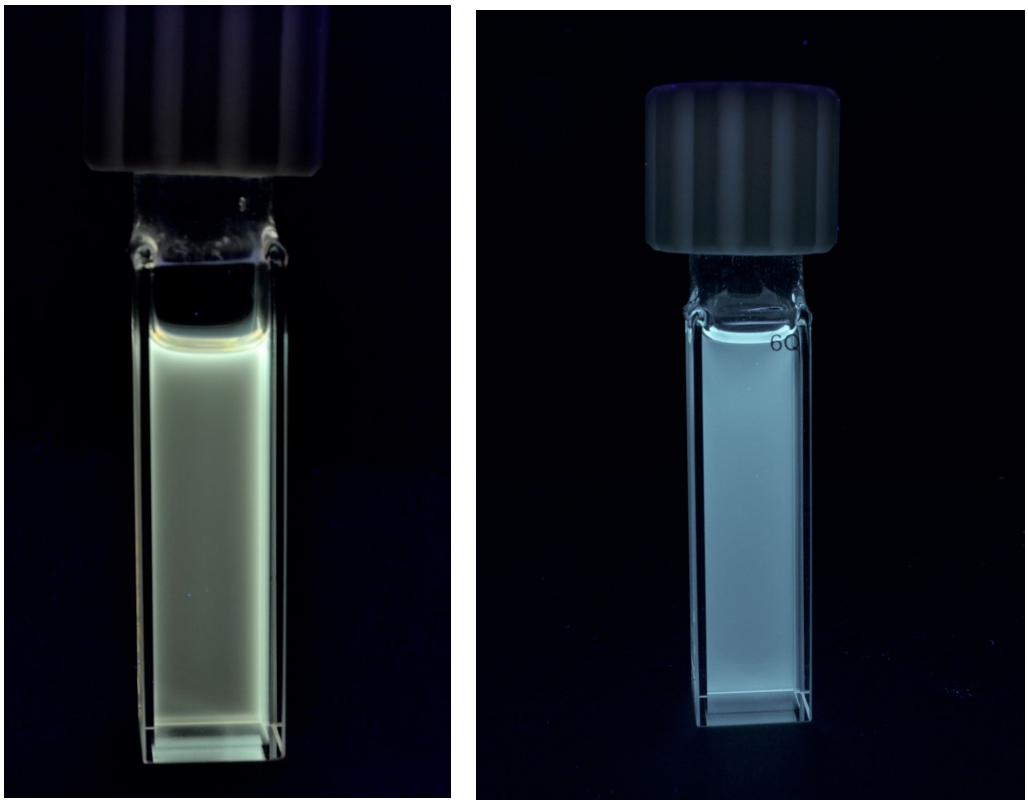

Figure S73: **SS2**, 10^{-5}M, air equilibrated (left) **SS2**, 10^{-5}M, deoxygenated solution (right), CH_2Cl_2, r.t; λ_{exc}= 365 nm.

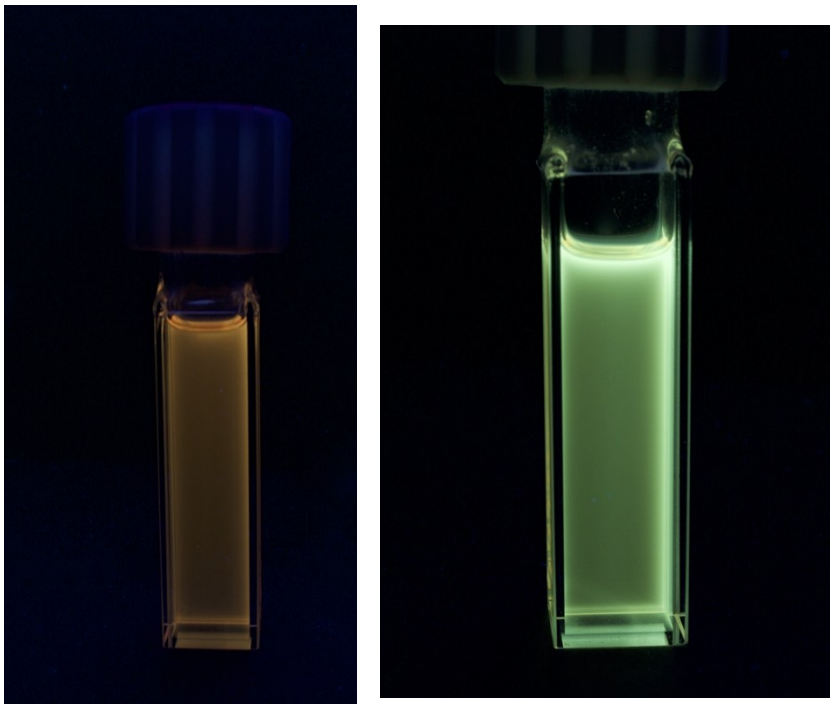

[i]G. A. Crosby and J. N. Demas, *J. Phys. Chem.* 1971, **75**, 991-1024.

[ii]D. F. Eaton, *Pure Appl. Chem.* 1988, **60**, 1107-1114.

[iii]K. Nakamura, *Bull. Chem. Soc. Jpn.* 1982, **55**, 2697–2705.

[iv]R. N. Butler, Tetrazoles. In "*Comprehensive Heterocyclic Chemistry II*"; Storr, R. C., Ed.; Pergamon Press: Oxford, U.K., 1996; Vol. **4**, 621-678, and references cited therein.

[vi] K. Koguro, T. Oga, S. Mitsui and R. Orita, *Synthesis* 1998, **910-**914.

[vii] S. Stagni, S. Colella, A. Palazzi, G. Valenti, S. Zacchini, F. Paolucci, M. Marcaccio, R. Q. Albuquerque and L. De Cola, *Inorg. Chem.*, 2008, **47**, 10509-10521.

[viii] D. M. Jameson, *Introduction to Fluorescence*; CRC Press: Boca Raton, FL, 2014.